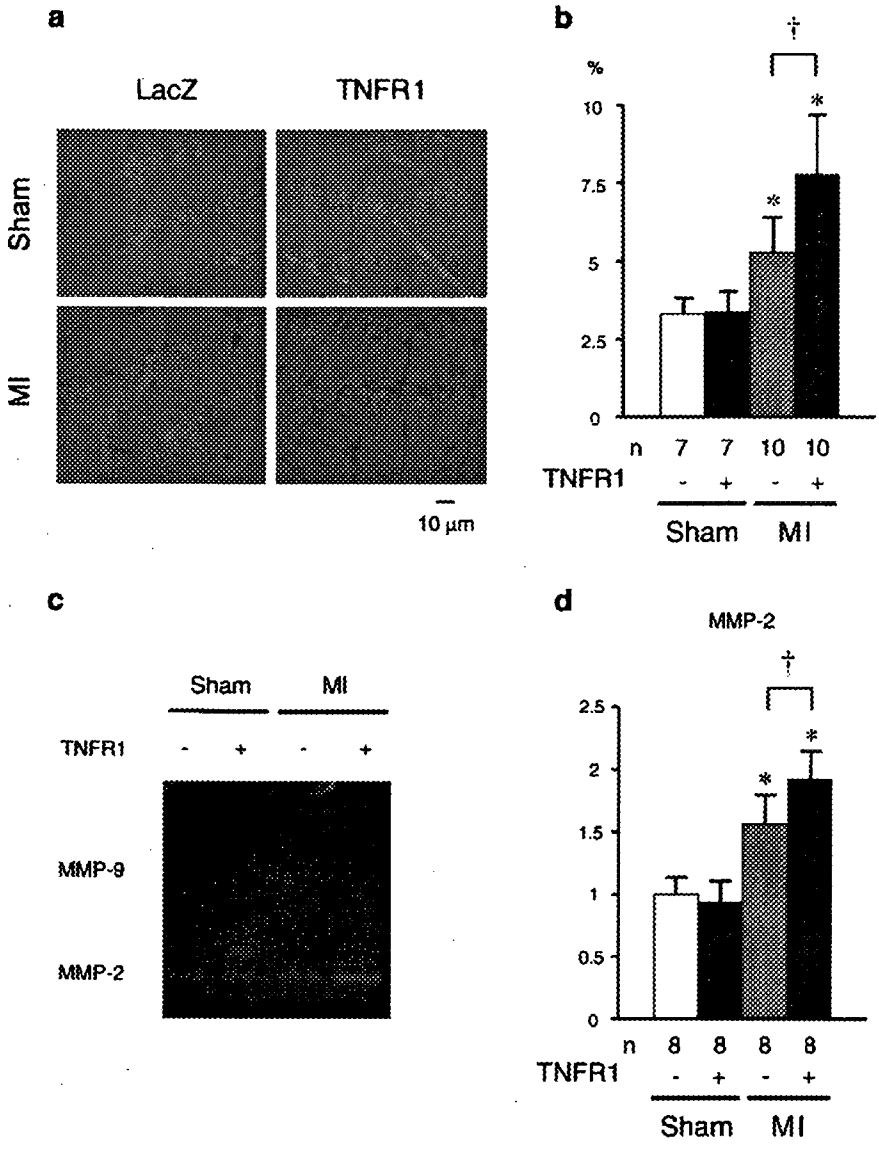

Fig. 7. Collagen volume analysis of the non-infarct myocardium on day 28 after MI: representative micrographs of Picrosirius red staining (a) and summarized data for collagen volume fraction (b). Gelatin zymography for MMP-2 and MMP-9 in non-infarct myocardium on day 28 after MI: representative gel (c) and summarized data for densitometric analysis (d). Each value is expressed as the ratio to the average of MMP-2 in Sham/LacZ mice. Values are mean±SD. TNFR1 (−) indicates post-MI treatment with AdLacZ; TNFR1 (+), post-MI treatment with AdTNFR1; Sham, sham-operated mice; MI, coronary ligated mice. *$p<0.05$ vs. Sham/LacZ mice, †$p<0.05$ vs. MI/LacZ mice.

augmented significantly in MI/TNFR1 mice. Both LV dP/dt_{max} and LV dP/dt_{min}, which decreased significantly in MI, were further lowered significantly by post-MI treatment with soluble TNF receptors. Although body weight was similar among 4 groups, LV weight/body weight ratio increased significantly in MI and further exacerbated with TNFR1 treatment. Along with increased LV end-diastolic pressure, lung weight/body weight ratio also increased significantly in MI/LacZ mice with further increment by TNFR1 treatment. These results suggest that the post-MI treatment with soluble TNF receptors exacerbates ventricular remodeling and pulmonary congestion after MI.

3.2.2. Enhanced fibrosis in non-infarct myocardium with further activation of MMP-2

Collagen was visualized in LV cross-section using Picrosirius red staining (Fig. 7a). As summarized in Fig. 7b, collagen volume fraction, which increased in non-infarct myocardium of MI/LacZ mice, was further augmented significantly by TNFR1 treatment. To further elucidate the mechanisms of increased myocardial fibrosis in MI/TNFR1 mice, MMP-2 and -9 activities were evaluated in non-infarct myocardium on day 28 using gelatin zymography (Fig. 7c). As summarized in Fig. 7d, MMP-2 activity increased significantly

after MI and was further activated by TNFR1 treatment, although MMP-9 activity was not altered.

These results indicate that post-MI treatment with soluble TNF receptors exacerbates ventricular dysfunction and remodeling, with enhanced fibrosis and further activation of MMP-2 in non-infarct myocardium.

4. Discussion

Proinflammatory cytokines including TNF-α have been implicated in the pathogenesis of cardiovascular diseases [6,7]. However, the roles of these cytokines in myocardial infarction remain controversial. In the present study, we evaluated the effects of soluble TNF receptor treatment on MI. Treatment with soluble TNFR1 neutralized the bioactivity of TNF-α that was activated after MI, and prevented apoptosis of infiltrating cells in the infarct myocardium. However, pre-MI treatment with soluble TNFR1 promoted ventricular rupture by reducing fibrosis with further activation of MMP-9. Furthermore, post-MI treatment with soluble TNFR1 exacerbated ventricular dysfunction and remodeling, and enhanced fibrosis in non-infarct myocardium with further activation of MMP-2. Because both pre- and post-MI treatments with soluble TNFR1 were deleterious in a mouse model of MI, TNF-α may play some protective roles in MI.

We used AdTNFR1 to block the effects of TNF-α after MI. We have previously confirmed the efficacy of AdTNFR1 treatment in transgenic mice with cardiac-specific overexpression of TNF-α [18]. Injection of 10^9 pfu of AdTNFR1 increased plasma levels of soluble TNFR1 substantially and ameliorated myocardial inflammation induced by TNF-α overexpression for 6 weeks [18]. In the present study, pro-inflammatory cytokines and chemokines including TNF-α, IL-1β, IL-6, TGF-β, MCP-1, and RANTES were up-regulated in infarct myocardium 3 days after coronary ligation. Pre-MI treatment with AdTNFR1 increased plasma levels of soluble TNFR1 as previously reported [18]. Although AdTNFR1 treatment did not affect the transcript levels of proinflammatory cytokines and chemokines, it significantly blocked the bioactivity of TNF-α in infarct myocardium. These results indicate that treatment with AdTNFR1 neutralizes the effects of TNF-α induced after MI. Furthermore, induction of proinflammatory cytokines and chemokines in infarct myocardium is not solely mediated by TNF-α.

Cardiac rupture is an acute fatal complication that occurs during the early phase after MI. Disorganized infarct healing and the resultant deficiency or disruption of extracellular matrix (ECM) at the infarction site may lead to myocardial rupture. In the present study, we have shown that pre-MI treatment with soluble TNFR1 increases ventricular rupture after MI without affecting systemic blood pressure or heart rate, but significantly reduced collagen content of infarct myocardium with further MMP-9 activation. Because targeted disruption of MMP-9 is known to prevent ventricular rupture after MI [22], further activation of MMP-9 may be the primary cause of increased ventricular rupture in this mouse MI model. Further activation of MMP-9 may be attributed to increased macrophages in soluble TNFR1-treated infarct myocardium, because macrophages produce substantial amounts of MMP-9 [21]. Increased macrophages may result from the anti-apoptotic effects of soluble TNFR1, because apoptosis of infiltrating cells was significantly attenuated by the treatment. These results suggest that TNF-α may be necessary for proper coordination of tissue repair processes after MI.

TNF-α is a potent inducer of apoptosis in a variety of cells including macrophages and myocytes [5,20]. In the present study, we have demonstrated that treatment with soluble TNFR1 decreases the number of apoptotic cells in infarct myocardium 3 days after MI, which is consistent with the blockade of TNF-α bioactivity by the treatment. Most of the apoptotic cells were interstitial infiltrating cells including macrophages, rather than myocytes. Because the number of infiltrating cells was not different between AdLacZ- and AdTNFR1-treated infarct myocardium 1 day after MI, the increase in relative number of macrophages in AdTNFR1-treated infarct myocardium after 3 days was probably due to decreased apoptosis of infiltrating cells. In contrast, Kurrelmeyer et al. [15] reported that targeted disruption of both TNFR1 and TNFR2 increased the size of infarct myocardium by enhancing apoptosis of cardiac myocytes within 24 h after MI, suggesting that TNF-α may protect cardiac myocytes from ischemic injury by preventing apoptosis. Furthermore, pre-MI treatment with TNF-α has been shown to ameliorate ischemic/reperfusion injury with induction of MnSOD [23]. These results suggest that the pathophysiological roles of TNF-α in the subacute phase of MI (more than 3 days) may be different from those in acute ischemia (within 24 h). TNF-α may protect cardiac myocytes from cell death in acute ischemia, but promote apoptosis of infiltrating cells to resolve inflammation in the subacute phase.

Myocardial infarction leads to complex structural alterations in both infarct and non-infarct myocardium, resulting in progressive dilatation and dysfunction of the ventricle (remodeling). TNF-α is induced in the failing human heart [2]. Its role in the progression of ventricular remodeling is inferred from findings that TNF-α suppresses cardiac contractility [3], provokes myocardial hypertrophy [4], and induces apoptosis in cultured cardiac myocytes [5]. However, in the present study, treatment with soluble TNFR1 further exacerbated ventricular dysfunction and remodeling even when given after the acute phase. These results suggest that TNF-α may protect infarct and non-infarct myocardium from the progression of remodeling. The dynamics of synthesis and breakdown of ECM proteins play an important role in post-MI LV remodeling. In particular, increased expression and activation of MMPs have been implicated in this process [21]. Several studies have demonstrated that MMPs are involved not only in cardiac rupture [19,22] but also in LV remodeling and failure [24,25]. Among the known MMPs, MMP-2 and MMP-9 have been shown to play an important role in post-MI remodeling [19,24]. Although MMP-9 is

mainly expressed in infiltrating inflammatory cells such as neutrophils and macrophages, MMP-2 is ubiquitously distributed in cardiac myocytes and fibroblasts and is up-regulated after MI. In the present study, we have demonstrated that post-MI treatment with soluble TNFR1 further activates MMP-2 in non-infarct myocardium, while the pre-MI treatment augments MMP-9 in infarct myocardium. Furthermore, we have previously reported that targeted disruption of MMP-2 as well as MMP-9 attenuates not only ventricular rupture but also ventricular remodeling after MI [19]. Therefore, exacerbation of ventricular remodeling and dysfunction after TNFR1 treatment may be mediated by further activation of MMP-2, although the precise mechanism by which MMP-2 is further activated remains undetermined.

The present findings contradict the results of Sun et al. [12] using TNF-α knockout mice. Targeted disruption of TNF-α by gene knockout significantly reduced acute cardiac rupture and improved chronic left ventricular dysfunction after MI, accompanied by a reduction of cardiac inflammatory cell infiltration, cytokine expression, and MMP-9 activity. Chronically, TNF-α knockout mice also showed less fibrosis and apoptosis in the myocardium remote from the infarct zone, which contributed to improved ventricular function [12]. These results are thoroughly opposite to ours. Although gene targeting completely eliminated TNF-α in myocardium, the absence of TNF-α during embryogenesis and development may have altered other signaling pathways to secure physiological growth of these mice. Therefore, the differences between the present study and the previous report may be attributed to the methods adopted to block the effects of TNF-α.

TNF-α initiates its biological effects by binding two distinct cell surface receptors with approximate molecular masses of 55 kDa (TNFR1) and 75 kDa (TNFR2) [1]. Both receptors are expressed in most cell types, including cardiac myocytes. Although most biological activities of TNF-α are signaled through TNFR1, the role of TNFR2 remains unclear. Targeted disruption of TNFR1 has been shown to reduce ventricular rupture and remodeling after MI [13]. Furthermore Higuchi et al. [26] have recently demonstrated that ablation of TNFR1 ameliorated heart failure and improved survival while ablation of the TNFR2 gene exacerbated heart failure and reduced survival of TNF-α transgenic mice, suggesting a cardioprotective role of TNFR2-mediated signaling. Therefore, exacerbation of ventricular rupture and remodeling observed in the present study may have derived from blockade of TNFR2-mediated signaling. Because the dissociation constants of TNFR1 and TNFR2 are $2–5\times10^{-10}$ and $3–7\times10^{-11}$, respectively [1], high levels of TNF-α interact with both TNFR1 and TNFR2, while low levels may only stimulate TNFR2 pathways. In other words, low levels of soluble TNF receptors may only block cytotoxic TNFR1, whereas high levels of soluble TNF receptors may also block the protective TNFR2. Because plasma levels of soluble TNF receptors in the present study (about 500 μg/ml) were more than 100 times higher than clinical plasma levels (approximately 0.3–3 μg/ml) [27], these high levels may block the protective TNFR2 resulting in deleterious results. Using lower doses of soluble TNF receptors may produce different results.

Another explanation for the negative results of the present study might be intrinsic toxicity of soluble TNF receptors [7]. Soluble TNF receptor also acts as a carrier protein that stabilizes TNF-α resulting in the accumulation of high concentrations of immunoreactive TNF-α [18]. Because binding of TNF-α–TNFR complexes is reversible [28], the increase in level of TNF-α–TNFR complex may lead to an increase in the duration of TNF bioactivity. Specifically, this might be the case for soluble TNFR2 fusion proteins, including etanercept that was used in RENEWAL [8]. Studies of the binding of TNF-α with soluble TNF receptor fusion proteins have shown that TNFR2 exchanges bound TNF-α about 50- to 100-fold faster than TNFR1 [29]. Thus, although both fusion proteins in equilibrium bind TNF-α with high affinity, the TNF-α–TNFR1 fusion protein complex is kinetically more stable than the TNFR2 fusion construct. Because the soluble TNF receptors used in the present study were TNFR1, the intrinsic toxicity might have been less than that if TNFR2 were used. To confirm this hypothesis, we measured the bioactivity of TNF-α in the myocardium, and found that the bioactivity was significantly reduced by the treatment. Therefore, this might not be the case in the present study.

Although the negative results of anti-TNF clinical trials in patients with heart failure prompted us to conduct the present study, there are several important aspects that are different between the present study and the clinical trials. First, acute myocardial infarction was used as a model of heart failure in the present study, while patients with chronic heart failure were recruited in the clinical trials. The roles of proinflammatory cytokines might be different in acute and chronic phases of myocardial infarction. Second, the dosage of soluble TNF receptors used in the present study was more than 100 times higher than that used in the clinical trials. Effects of high doses should be different from those of lower doses, which remain undetermined in this mouse MI model. Therefore, caution has to be exercised in interpreting the present results in association with the clinical trials.

In conclusion, treatment with soluble TNF receptors increases ventricular rupture and exacerbates cardiac remodeling in a murine model of MI. Because TNF-α seems to play both cytotoxic and protective roles in cardiovascular diseases, further studies are required to elucidate the optimal approach to modulate proinflammatory cytokines in clinical practice.

Acknowledgments

A part of this study was conducted in Kyushu University Station for Collaborative Research. This study was supported by a grant from Kimura Memorial Heart Foundation, by the Grant for Research on Cardiovascular Disease from Japan Heart Foundation/Pfizer Pharmaceuticals Inc., by the Grant-in-Aid for Scientific Research from the Japan Society for the promotion of Science (C15590755), by the Health and

Labour Sciences Research Grant for Research on Advanced Medical Technology from the Ministry of Health, Labour and Welfare of Japan (H14-Nano-002), by the Health and Labour Sciences Research Grant for Research on Medical Devices for Analyzing, Supporting and Substituting the Function of Human Body from the Ministry of Health, Labour and Welfare of Japan (H15-Physi-001), and by the Health and Labour Sciences Research Grant for Research on Measures for Intractable Disease from the Ministry of Health, Labour and Welfare of Japan (H17-Nanchi-22).

References

[1] Wang H, Czura CJ, Tracey KJ. Tumor necrosis factor. In: Thomson AW, Lotze MT, editors. The cytokine handbook. 4th ed. San Diego: Academic Press; 2003. p. 837–60.
[2] Torre-Amione G, Kapadia S, Lee J, Durand JB, Bies RD, Young JB, et al. Tumor necrosis factor-alpha and tumor necrosis factor receptors in the failing human heart. Circulation 1996;93:704–11.
[3] Finkel MS, Oddis CV, Jacob TD, Watkins SC, Hattler BG, Simmons RL. Negative inotropic effects of cytokines on the heart mediated by nitric oxide. Science 1992;257:387–9.
[4] Yokoyama T, Nakano M, Bednarczyk JL, McIntyre BW, Entman M, Mann DL. Tumor necrosis factor-alpha provokes a hypertrophic growth response in adult cardiac myocytes. Circulation 1997;95:1247–52.
[5] Krown KA, Page MT, Nguyen C, Zechner D, Gutierrez V, Comstock KL, et al. Tumor necrosis factor alpha-induced apoptosis in cardiac myocytes. Involvement of the sphingolipid signaling cascade in cardiac cell death. J Clin Invest 1996;98:2854–65.
[6] Feldman AM, Combes A, Wagner D, Kadokami T, Kubota T, Li YY, et al. The role of tumor necrosis factor in the pathophysiology of heart failure. J Am Coll Cardiol 2000;35:537–44.
[7] Mann DL. Inflammatory mediators and the failing heart: past, present, and the foreseeable future. Circ Res 2002;91:988–98.
[8] Mann DL, McMurray JJ, Packer M, Swedberg K, Borer JS, Colucci WS, et al. Targeted anticytokine therapy in patients with chronic heart failure: results of the Randomized Etanercept Worldwide Evaluation (RENEWAL). Circulation 2004;109:1594–602.
[9] Chung ES, Packer M, Lo KH, Fasanmade AA, Willerson JT. Randomized, double-blind, placebo-controlled, pilot trial of infliximab, a chimeric monoclonal antibody to tumor necrosis factor-alpha, in patients with moderate-to-severe heart failure: results of the anti-TNF Therapy Against Congestive Heart Failure (ATTACH) trial. Circulation 2003;107:3133–40.
[10] Hayashidani S, Tsutsui H, Shiomi T, Ikeuchi M, Matsusaka H, Suematsu N, et al. Anti-monocyte chemoattractant protein-1 gene therapy attenuates left ventricular remodeling and failure after experimental myocardial infarction. Circulation 2003;108:2134–40.
[11] Sugano M, Tsuchida K, Hata T, Makino N. In vivo transfer of soluble TNF-alpha receptor 1 gene improves cardiac function and reduces infarct size after myocardial infarction in rats. FASEB J 2004;18:911–3.
[12] Sun M, Dawood F, Wen WH, Chen M, Dixon I, Kirshenbaum LA, et al. Excessive tumor necrosis factor activation after infarction contributes to susceptibility of myocardial rupture and left ventricular dysfunction. Circulation 2004;110:3221–8.
[13] Ramani R, Mathier M, Wang P, Gibson G, Togel S, Dawson J, et al. Inhibition of tumor necrosis factor receptor-1-mediated pathways has beneficial effects in a murine model of postischemic remodeling. Am J Physiol Heart Circ Physiol 2004;287:H1369–77.
[14] Hwang MW, Matsumori A, Furukawa Y, Ono K, Okada M, Iwasaki A, et al. Neutralization of interleukin-1beta in the acute phase of myocardial infarction promotes the progression of left ventricular remodeling. J Am Coll Cardiol 2001;38:1546–53.
[15] Kurrelmeyer KM, Michael LH, Baumgarten G, Taffet GE, Peschon JJ, Sivasubramanian N, et al. Endogenous tumor necrosis factor protects the adult cardiac myocyte against ischemic-induced apoptosis in a murine model of acute myocardial infarction. Proc Natl Acad Sci U S A 2000;97:5456–61.
[16] Ikeuchi M, Tsutsui H, Shiomi T, Matsusaka H, Matsushima S, Wen J, et al. Inhibition of TGF-beta signaling exacerbates early cardiac dysfunction but prevents late remodeling after infarction. Cardiovasc Res 2004;64:526–35.
[17] Fuchs M, Hilfiker A, Kaminski K, Hilfiker-Kleiner D, Guener Z, Klein G, et al. Role of interleukin-6 for LV remodeling and survival after experimental myocardial infarction. FASEB J 2003;17:2118–20.
[18] Kubota T, Bounoutas GS, Miyagishima M, Kadokami T, Sanders VJ, Bruton C, et al. Soluble tumor necrosis factor receptor abrogates myocardial inflammation but not hypertrophy in cytokine-induced cardiomyopathy. Circulation 2000;101:2518–25.
[19] Hayashidani S, Tsutsui H, Ikeuchi M, Shiomi T, Matsusaka H, Kubota T, et al. Targeted deletion of MMP-2 attenuates early LV rupture and late remodeling after experimental myocardial infarction. Am J Physiol Heart Circ Physiol 2003;285:H1229–35.
[20] Kubota T, Miyagishima M, Frye CS, Alber SM, Bounoutas GS, Kadokami T, et al. Overexpression of tumor necrosis factor-alpha activates both anti- and pro-apoptotic pathways in the myocardium. J Mol Cell Cardiol 2001;33:1331–44.
[21] Li YY, Feng Y, McTiernan CF, Pei W, Moravec CS, Wang P, et al. Downregulation of matrix metalloproteinases and reduction in collagen damage in the failing human heart after support with left ventricular assist devices. Circulation 2001;104:1147–52.
[22] Heymans S, Luttun A, Nuyens D, Theilmeier G, Creemers E, Moons L, et al. Inhibition of plasminogen activators or matrix metalloproteinases prevents cardiac rupture but impairs therapeutic angiogenesis and causes cardiac failure. Nat Med 1999;5:1135–42.
[23] Wong GH, Goeddel DV. Induction of manganous superoxide dismutase by tumor necrosis factor: possible protective mechanism. Science 1988;242:941–4.
[24] Ducharme A, Frantz S, Aikawa M, Rabkin E, Lindsey M, Rohde LE, et al. Targeted deletion of matrix metalloproteinase-9 attenuates left ventricular enlargement and collagen accumulation after experimental myocardial infarction. J Clin Invest 2000;106:55–62.
[25] Rohde LE, Ducharme A, Arroyo LH, Aikawa M, Sukhova GH, Lopez-Anaya A, et al. Matrix metalloproteinase inhibition attenuates early left ventricular enlargement after experimental myocardial infarction in mice. Circulation 1999;99:3063–70.
[26] Higuchi Y, McTiernan CF, Frye CB, McGowan BS, Chan TO, Feldman AM. Tumor necrosis factor receptors 1 and 2 differentially regulate survival, cardiac dysfunction, and remodeling in transgenic mice with tumor necrosis factor-alpha-induced cardiomyopathy. Circulation 2004;109:1892–7.
[27] Deswal A, Bozkurt B, Seta Y, Parilti-Eiswirth S, Hayes FA, Blosch C, et al. Safety and efficacy of a soluble P75 tumor necrosis factor receptor (Enbrel, etanercept) in patients with advanced heart failure. Circulation 1999;99:3224–6.
[28] Frishman JI, Edwards III CK, Sonnenberg MG, Kohno T, Cohen AM, Dinarello CA. Tumor necrosis factor (TNF)-alpha-induced interleukin-8 in human blood cultures discriminates neutralization by the p55 and p75 TNF soluble receptors. J Infect Dis 2000;182:1722–30.
[29] Evans TJ, Moyes D, Carpenter A, Martin R, Loetscher H, Lesslauer W, et al. Protective effect of 55- but not 75-kD soluble tumor necrosis factor receptor-immunoglobulin G fusion proteins in an animal model of gram-negative sepsis. J Exp Med 1994;180:2173–9.

Significance of Asymmetric Basal Posterior Wall Thinning in Patients With Cardiac Fabry's Disease

Makoto Kawano, MD[a], Toshihiro Takenaka, MD[a], Yutaka Otsuji, MD[a,*], Hiroyuki Teraguchi, MD[a], Shiro Yoshifuku, MD[a], Toshinori Yuasa, MD[a], Bo Yu, MD[a], Masaaki Miyata, MD[a], Shuichi Hamasaki, MD[a], Shinichi Minagoe, MD[a], Yuichi Kanmura, MD[b], and Chuwa Tei, MD[a]

Although classic Fabry's disease results in multiple causes of death, the cardiac variant of Fabry's disease affects only the cardiac system and results in initial symmetric left ventricular (LV) hypertrophy and later LV dysfunction, asymmetric basal posterior LV wall thinning, restrictive mitral flow, and functional mitral regurgitation with end-stage chronic heart failure (CHF), leading to death. The purpose of this study was to investigate whether these findings predict prognoses in patients with cardiac Fabry's disease. In 13 consecutive men with cardiac Fabry's disease, LV wall thickness, the ejection fraction, mitral E-wave deceleration time, the LV Tei index, and functional mitral regurgitation were measured by echocardiography. Patients were followed for 5 to 96 months (mean 41 ± 9). Eight patients developed New York Heart Association class III CHF, and 6 experienced cardiac death. A LV Tei index >0.60 and basal posterior LV wall thinning with a ratio of ventricular septal to posterior wall thickness >1.3 significantly preceded CHF and death (Tei index: 4.4 and 5.1 years; posterior wall thinning: 4.0 and 4.7 years), respectively ($p < 0.05$). In conclusion, an increased LV Tei index and asymmetric basal posterior LV wall thinning are important echocardiographic findings that precede CHF and cardiac death in patients with cardiac Fabry's disease. **(Am J Cardiol 2007;99:261–263)**

Patients with classic Fabry's disease show multiple organ involvement, leading to heterogenous causes of death.[1,2] In contrast, an atypical variant of Fabry's disease with manifestations limited to the heart, reported as cardiac Fabry's disease,[3,4] is more frequent than previously expected and can be found in 3% to 6% of men with left ventricular (LV) hypertrophy.[5,6] We have empirically observed that patients with cardiac Fabry's disease initially present with symmetric LV hypertrophy without chronic heart failure (CHF) but later show LV dysfunction, asymmetric LV basal posterior wall thinning without ventricular septal thinning, restrictive mitral flow, and functional mitral regurgitation with end-stage CHF and cardiac death. The purpose of this study was to investigate the natural history of these findings and to characterize predictors of New York Heart Association (NYHA) class III CHF or cardiac death in patients with cardiac Fabry's disease.

Methods and Results

Four hundred fifty consecutive patients with ventricular septal or posterior wall thickness ≥13 mm were screened by the measurement of plasma α-galactosidase A activity from 1992 to 1996 at our institution, and 13 men were diagnosed with cardiac Fabry's disease using the following criteria:

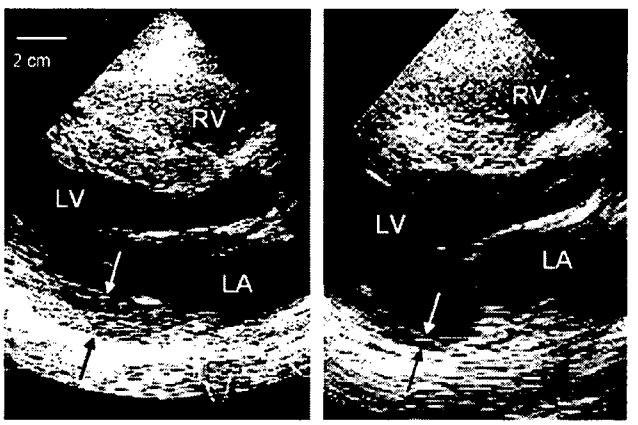

Figure 1. Serial echocardiograms of a patient with cardiac Fabry's disease at 57 *(left)* and 63 *(right)* years old. Ventricular septal and posterior wall thicknesses changed from 21 and 18 to 19 and 7 mm, respectively, with the development of CHF. LA = left atrium; LV = left ventricle; RV = right ventricle.

(1) low plasma α-galactosidase A activity (<4.5 nmol/hour/ml)[5]; (2) ventricular septal and/or posterior wall thickness ≥13 mm; (3) no clinical features of classic Fabry's disease, including angiokeratoma, acroparesthesia, hypohidrosis, and corneal opacity; and (4) accumulation of glycosphingolipid in biopsied cardiomyocytes and/or α-galactosidase A gene abnormalities.[7] These patients were followed for 41 ± 9 months by serial echocardiography, with intervals of 1 to 24 months (mean 3.3 ± 1.1). Clinical profiles are listed in Table 1. Coronary angiographic results were normal, and written informed consent was obtained from all patients.

Ventricular septal and posterior wall thicknesses were

Departments of [a]Cardiovascular, Respiratory and Metabolic Medicine and [b]Anesthesiology and Critical Care Medicine, Graduate School of Medicine, Kagoshima University, Kagoshima, Japan. Manuscript received January 23, 2006; revised manuscript received and accepted July 27, 2006.

*Corresponding author: Tel: 81-99-275-5318; fax: 81-99-265-8447.
E-mail address: otsujiy@med.uoeh-u.ac.jp (Y. Otsuji).

0002-9149/07/$ – see front matter
doi:10.1016/j.amjcard.2006.07.088

Table 1
Clinical, enzymatic, pathologic, and genetic characteristics of patients

No.	Age at Diagnosis (yrs)	Previous Diagnosis	Plasma α-gal A Activity (nmol/h/ml)	Accumulation in Myocyte	Gene Abnormality	Age at NYHA Class III (yrs)	Duration of Follow-Up (mo)	Age at Death (yrs)
1	47	HC	1.5	+	NE	NYHA <III	20	Alive
2	57	HC	0.4	+	A20P	62	85	64
3	60	HC	1.0	0	F229L	NYHA <III	16	Alive
4	62	HC	1.2	+	Decreased mRNA	67	76	68
5	62	HC	1.3	+	NE	63	25	64
6	66	HC	0.9	+	NE	66	7	66
7	70	HC	0.6	+	Decreased mRNA	73	40	74
8	71	HC	1.4	+	NE	73	46	Alive
9	71	HC	0.7	+	Decreased mRNA	75	55	76
10	74	HC	1.0	+	NE	NYHA <III	6	Alive
11	79	HC	0.6	NE	Decreased mRNA	80	96	Alive
12	43	HHD	1.1	+	NE	NYHA <III	5	Alive
13	62	HHD	0.6	+	M296I	NYHA <III	58	Alive

α-gal A = α-galactosidase A; HC = hypertrophic cardiomyopathy; HHD = hypertensive heart disease; mRNA = messenger ribonucleic acid; NE = not examined.

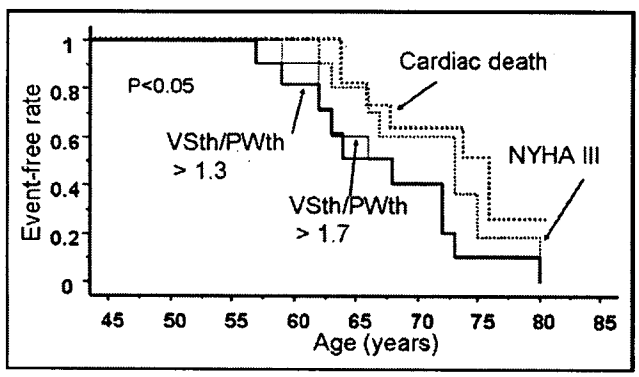

Figure 2. Kaplan-Meier curves showing that ventricular septum/posterior wall thickness ratio (VSth/PWth) >1.3 and 1.7 significantly preceded NYHA class III CHF and cardiac death in patients with cardiac Fabry's disease.

measured with echocardiography, and their ratio was calculated, with 1.2 defined as the upper limit of normal.[8] The LV ejection fraction was measured by the biplane Simpson's method, and left atrial dimension was measured by M-mode echocardiography. A mitral flow restrictive filling pattern was defined as an E/A ratio >2 and E-wave deceleration time <150 ms.[9] The Tei index, combining systolic and diastolic function, was obtained by mitral filling and aortic ejection flow.[10] Mitral regurgitant volume was quantified by Doppler echocardiography.

Statistical analysis was performed using StatView version 5.0 (SAS Institute Inc., Cary, North Carolina). Clinical and echocardiographic data after the introduction of enzymatic replacement therapy were excluded from analysis. The event-free rate from the ventricular septum/posterior wall thickness ratio >1.3, 1.5, 1.7, or 1.9; LV ejection fraction <50%; left atrial dimension >40 mm; restrictive mitral flow; Tei index >0.50, 0.60, 0.70, or 0.80; mitral regurgitant fraction >30%; NYHA class III; and cardiac death was calculated using the Kaplan-Meier method. A p value <0.05 was considered significant.

NYHA class III or IV CHF developed in 8 of the 13 patients during follow-up. Six died, and the cause was CHF in all 6 patients. Most patients with CHF demonstrated (1) LV systolic and diastolic dysfunction, with reduced ejection fractions, shortened mitral E-wave deceleration times, and increased Tei indexes; (2) left atrial dilation; (3) asymmetric basal posterior LV wall thinning (Figure 1); and (4) significant mitral regurgitation. The ages at the development of these findings are listed in Table 2.

Among the evaluated echocardiographic events, Kaplan-Meier analysis identified significant associations with progression to NYHA class III CHF and cardiac death for a Tei index >0.60 and ventricular septum/posterior wall thickness ratio >1.3, 1.5, and 1.7 (Figure 2). A Tei index >0.60 preceded NYHA class III CHF and death by 4.4 and 5.1 years ($p < 0.05$), respectively. Ventricular septum/posterior wall thickness ratio >1.3, 1.5, or 1.7 significantly preceded NYHA class III CHF and cardiac death by 4.0, 3.8, or 3.4 and 4.7, 4.5, or 4.1 years ($p < 0.05$), respectively.

Discussion

This study demonstrated that an increased Tei index and LV basal posterior wall thinning were significantly associated with progression to NYHA class III CHF and cardiac death in patients with cardiac Fabry's disease. Other findings, such as a reduced LV ejection fraction, restrictive mitral flow, left atrial dilation, and significant mitral regurgitation, occurred temporally close to the development of CHF or cardiac death and were unable to predict disease progression by Kaplan-Meier analysis. These results may lead to a better understanding of the natural history of cardiac Fabry's disease and better timing to start enzymatic replacement or gene therapy.[11–14]

The Tei index enables the prediction of outcomes in patients with cardiac amyloidosis and other diseases.[15] Basal posterior LV wall thinning and fibrosis have also been reported in patients with cardiac involvement in classic Fabry's disease.[16,17] The findings of the present study are consistent with these and further demonstrate that an increased Tei index and asymmetric LV basal posterior wall thinning are associated with progression to

Table 2
Age at event occurrence

No.	Echocardiographic Events												Clinical Events	
	LV Tei Index				VS/PW				LAD >40 mm	LVEF <50%	Restrictive Mitral Flow	MR Fraction >30%	NYHA Class III	Cardiac Death
	>0.50	>0.60	>0.70	>0.80	>1.3	>1.5	>1.7	>1.9						
1	49	49	NE	NE	NE	NE	NE	NE	49	NE	NE	NE	NE	NE
2	57	60	60	60	59	59	59	60	59	59	62	62	62	64
3	60	60	60	NE	NE	NE	NE	NE	NE	NE	NE	NE	NE	NE
4	65	65	65	67	63	63	63	63	66	63	66	68	67	68
5	62	62	62	62	57	57	62	62	62	62	63	64	63	64
6	66	66	66	66	64	66	66	66	66	66	66	66	66	66
7	73	73	73	73	73	73	73	73	73	73	73	73	73	74
8	72	72	73	73	68	68	68	71	73	71	73	NE	73	NE
9	75	75	75	75	72	72	72	72	75	75	75	75	75	76
10	74	74	74	NE	72	72	72	NE	74	74	NE	NE	NE	NE
11	80	80	80	NE	80	80	80	80	80	80	80	NE	80	NE
12	43	NE	NE	NE	NE	NE	NE	NE	43	NE	NE	NE	NE	NE
13	66	66	NE	NE	62	62	66	66	NE	66	NE	NE	NE	NE
Mean	64.8	66.8	69.4	70.0	67.2	67.4	67.8	69.4	68.3	69.0	70.6	70.7	71.2	71.9
SE	3.0	2.5	2.1	1.9	2.2	2.2	2.0	2.2	2.9	2.1	2.0	1.7	2.1	1.7

Means and SEs were obtained by the Kaplan-Meier method.

EF = ejection fraction; LAD = left atrial dimension; MR = mitral regurgitation; NE = no event throughout the observation; PW = posterior wall thickness; VS = ventricular septal thickness.

CHF and cardiac death in patients with cardiac Fabry's disease.

Although the incidence of cardiac Fabry's disease is more common than previously believed,[5,6] its incidence and the utility of screening in patients with LV hypertrophy need to be established with a large number of patients. A Tei index >0.60 and LV basal posterior wall thinning were associated with progression to CHF and cardiac death in patients with cardiac Fabry's disease, whose causes of death were uniformly cardiac. However, the results may not be generalized to classic Fabry's disease with heterogenous causes of death. Tissue Doppler imaging and the Tei index may allow the earlier and better prediction of cardiac Fabry's disease before the development of structural abnormalities,[18] which requires further investigation.

1. Desnick RJ, Ioannou YA, Eng CM. α-Galactosidase A deficiency: Fabry disease. In: Scriver CR, Beaudet AL, Sly WS, Valle D, eds. The Metabolic and Molecular Basis of Inherited Disease, Vol. 3. 8th Ed. New York, New York: McGraw-Hill, 2001:3733–3774.
2. Desnick RJ, Brady R, Barranger J, Collins AJ, Germain DP, Goldman M, Grabowski G, Packman S, Wilcox WR. Fabry disease, an under-recognized multisystemic disorder: expert recommendations for diagnosis, management, and enzyme replacement therapy. *Ann Intern Med* 2003;138:338–346.
3. Elleder M, Bradová V, Šmíd F, Budešínsky, M, Harzer K, Kustermann-Kuhn B, Ledvinova J, Belohlavek, Kral V, Dorazilova V. Cardiocyte storage and hypertrophy as a sole manifestation of Fabry's disease. Report on a case simulating hypertrophic non-obstructive cardiomyopathy. *Virchows Arch A Pathol Anat Histopathol* 1990;417:449–455.
4. von Scheidt W, Eng CM, Fitzmaurice TF, Erdmann E, Hübner G, Olsen EGJ, Christomanou H, Kandolf R, Bishop DF, Desnick RJ. An atypical variant of Fabry's disease with manifestations confined to the myocardium. *N Engl J Med* 1991;324:395–399.
5. Nakao S, Takenaka T, Maeda M, Kodama C, Tanaka A, Tahara M, Yoshida A, Kuriyama M, Hayashibe H, Sakuraba H, Tanaka H. An atypical variant of Fabry's disease in men with left ventricular hypertrophy. *N Engl J Med* 1995;333:288–293.
6. Sachdev B, Takenaka T, Teraguchi H, Tei C, Lee P, McKenna WJ, Elliott PM. Prevalence of Anderson-Fabry disease in male patients with late onset hypertrophic cardiomyopathy. *Circulation* 2002;105:1407–1411.
7. Yoshitama T, Nakao S, Takenaka T, Teraguchi H, Sasaki T, Kodama C, Tanaka A, Kisanuki A, Tei C. Molecular genetic, biochemical, and clinical studies in three families with cardiac Fabry's disease. *Am J Cardiol* 2001;87:71–75.
8. Henry WL, Clark CE, Epstein SE. Asymmetric septal hypertrophy: echocardiographic identification of the pathognomonic anatomic abnormality of IHSS. *Circulation* 1973;47:225–233.
9. Cohen GI, Pietrolungo JF, Thomas JD, Klein AL. A practical guide to assessment of ventricular diastolic function using Doppler echocardiography. *J Am Coll Cardiol* 1996;27:1753–1760.
10. Tei C. New non-invasive index for combined systolic and diastolic ventricular function. *J Cardiol* 1995;26:135–136.
11. Eng CM, Guffon N, Wilcox WR, Germain DP, Lee P, Waldek S, Caplan L, Linthorst GE, Desnick RJ. Safety and efficacy of recombinant human α-galactosidase A replacement therapy in Fabry's disease. *N Engl J Med* 2001;345:9–16.
12. Schiffmann R, Murray GJ, Treco D, Daniel P, Sellos-Moura M, Myers M, Quirk JM, Zirzow E, Liang TJ, Kreps C, et al. Infusion of alpha-galactosidase A reduces tissue globotriaosylceramide storage in patients with Fabry disease. *Proc Natl Acad Sci USA* 2000;97:365–370.
13. Takenaka T, Murray GJ, Qin G, Quirk JM, Ohshima T, Qasba P, Clark K, Kulkarni AB, Brady RO, Medin JA. Long-term enzyme correction and lipid reduction in multiple organs of primary and secondary transplanted Fabry mice receiving transduced bone marrow cells. *Proc Natl Acad Sci U S A* 2000;97:7515–7520.
14. Yoshimitsu M, Sato T, Tao K, Walia JS, Rasaiah VI, Sleep GT, Murray GJ, Poeppl AG, Underwood J, West L, et al. Bioluminescent imaging of a marking transgene and correction of Fabry mice by neonatal injection of recombinant lentiviral vectors. *Proc Natl Acad Sci USA* 2004;101:16909–16914.
15. Tei C, Dujardin KS, Hodge DO, Kyle RA, Tajik AJ, Seward JB. Doppler index combining systolic and diastolic myocardial performance: clinical value in cardiac amyloidosis. *J Am Coll Cardiol* 1996;28:658–664.
16. Bass JL, Shrivastava S, Grabowski GA, Desnick RJ, Moller JH. The M-mode echocardiogram in Fabry's disease. *Am Heart J* 1980;100:807–812.
17. Moon JCC, Sachdev B, Elkington AG, McKenna WJ, Mehta A, Pennell DJ, Leed PJ, Elliott PM. Gadolinium enhanced cardiovascular magnetic resonance in Anderson-Fabry disease: evidence for a disease specific abnormality of the myocardial interstitium. *Eur Heart J* 2003;24:2151–2155.
18. Pieroni M, Chimenti C, Ricci R, Sale P, Russo MA, Frustaci A. Early detection of Fabry cardiomyopathy by tissue Doppler imaging. *Circulation* 2003;107:1978–1984.

Available online at www.sciencedirect.com
ScienceDirect
ELSEVIER
Biochemical and Biophysical Research Communications xxx (2008) xxx–xxx
BBRC
www.elsevier.com/locate/ybbrc

Which skeletal myoblasts and how to be transplanted for cardiac repair? ☆

Asaki Tezuka [a,1], Tomie Kawada [b,1], Mikio Nakazawa [c], Fujiko Masui [a], Satoshi Konno [d], Shin-ichi Nitta [d], Teruhiko Toyo-oka [a,e,*]

[a] *Department of Pathophysiology and Internal Medicine, University of Tokyo, Hongo 7-3-1, Bunkyo-ku, Tokyo 113-0033, Japan*
[b] *Department of Pharmacy, Niigata University Medical and Dental Hospital, Niigata 851-8520, Japan*
[c] *Division of Medical Technology, Department of Health Sciences, Faculty of Medicine, Niigata University 851-8510, Japan*
[d] *Division of Medical Engineering, Institute for Gerontology, Tohoku University, Seiryo 2-1, Aoba-ku, Sendai 980-8575, Japan*
[e] *Division of Molecular Cardiology, Department of Biofunctional Sciences, Tohoku University Bioengineering Organization (TUBERO), Seiryo 2-1, Aoba-ku, Sendai 980-8575, Japan*

Received 7 October 2007

Abstract

Clinical efficacy of skeletal myoblast (skMb) transplantation is controversial whether this treatment produces beneficial outcome in patients with dilated cardiomyopathy (DCM). Based on immunol- ogical tolerance between wild-type and DCM hamsters with the deletion of δ-sarcoglycan (SG) gene, skMb engraftment in TO-2 myocardium (3×10^5 cells in ~100 mg heart) was verified by the donor-specific expression of δ-SG transgene constitutively produced throughout myogenesis. At 5 weeks after the transplantation, the cell rates expressing fast-myosin heavy chain (MHC) exceeded slow-MHC in δ-SG^+ cells. Fifteen weeks after (corresponding to ~12 years in humans), fast MHC^+ cells nullified, but the δ-SG^+/slow MHC^+ cell number remained unaltered. These skMbs fused with host cardiomyocytes *via* connexin-43 and intercalated disc, modestly improving the hemodynamics without arrhythmia, when engrafted skMbs were sparsely disseminated in autopsied myocardium. These results provide us evidence that disseminating delivery of slow- MHC^+ myoblasts is promising for repairing DCM heart using histocompatible skeletal myoblasts in future.

Keywords: Cell transplantation; Skeletal myoblast; Fast-twitch muscle; Slow-twitch muscle; Dilated cardiomyopathy; δ-Sarcoglycan; Myosin heavy chain; Connexin-43; Intercalated disc; Fusion

DCM accounts for approximately one-half of clinical cases with advanced heart failure (AdHF). In spite of the steady progress in both basic and clinical researches, the prognosis of patients with DCM is still poor [1]. Cardiac transplantation is so far the most life-saving treatment of AdHF, though various sociomedical problems exist intrinsic to this treatment. Skeletal myoblast (skMb) transplantation has now reached a novel strategy for improving cardiac dysfunction secondary to ischemic injury [2–5], leaving clinical argument of arrhythmogenic substrate [6] or equivocal outcome in randomized and placebo-controlled study in MAGIC trial [7].

When a responsible gene causing DCM is identified, gene-targeted therapy using a long-lasting and non-harmful vector is one of the most promising options for preventing the progression from moderate cardiac dysfunction to AdHF [8]. This treatment might be less effective for restoring the necrotic cardiomyocytes. Though DCM is non-coronarogenic, the final pathway to AdHF would be common to ischemic heart disease [9–11]. SkMb transplantation

☆ This study was supported by grants from the Ministry of Education, Culture, Sports and Sciences, the Ministry of Health, Welfare and Labor, the Fugaku Research Foundation and the Motor Vehicle Foundation, Japan.

* Corresponding author. Address: Division of Molecular Cardiology, Department of Biofunctional Sciences, Tohoku University Bioengineering Organization (TUBERO), Seiryo 2-1, Aoba-ku, Sendai 980-8575, Japan. Fax: +81 22 717 7576.
E-mail address: toyooka-dmc@tubero.tohoku.ac.jp (T. Toyo-oka).
[1] These authors contributed equally to this work.

0006-291X/$ - see front matter © 2007 Published by Elsevier Inc.
doi:10.1016/j.bbrc.2007.11.084

after the gene normalization *ex vivo* would have the potential for supplementing adaptable cells in DCM heart where the original cardiomyocytes are already lost. TO-2 strain hamster is suitable for the study of human DCM, because the δ-SG gene is commonly deleted in both species with DCM [12–14] and similar clinical features are progressively shown including AdHF and sudden death [8,9,14].

Most studies on the cell-transplantation have employed immunosuppression procedures or immunodeficient animals to avoid rejection provoked in the recipients. As presented by δ-SG gene knockout mice, X-ray irradiation increased the number of donor-derived nuclei without advantage for the transgene expression [15]. Present study was focused following fundamental problems; (1) identification of promising cells among skMbs, (2) their efficient delivery and engraft- ment, using immunologically tolerant allografts from normal control to DCM hearts and (3) evaluation of physiological features of the engrafted heart after the short- and long-term follow-up.

Materials and methods

Because the space for this publication is limited, we shifted all sections for Experimental procedures to Supplementary Material. All statistical values are expressed by means ± SEM. Multiple groups were compared by one-way ANOVA followed by Bonferroni's post hoc test. *P* value below 0.05 was considered statistically significant.

Results and discussion

As a source of progenitor cells for cardiac muscle repair, a wide variety of stem cells have been reported, including skMb, cardiomyoblast, adipose tissue, and bone marrow cells, but it is still controversial whether the non-myogenic cells actually transdifferentiate to cardiomyocytes [16–18]. Considering clinical setting in the treatment of AdHF, all of these cells should be evaluated with great care to assure both their safety and efficacy. Selection of soleus muscle in the pioneer work by Taylor et al. was very appropriate for the skMb transplantation, because slow-twitch muscle fibers are preferentially present in this muscle [2]. When the life-threatening arrhythmias are avoided [5,6], skMb might be the most promising for the clinical application among these candidate tissues, because human studies have already shown a clear improvement of cardiac failure after myocardial infarction [3] and successful engraftment within a scar [4]. Other progenitor cells are attractive but still remain at an experimental stage [19]. The cause of discrepancy between two phase I studies [20,21] on intracoronary injection trial of bone marrow-derived progenitor cells in acute myocardial infarction may be explained by the heterogeneity of administered cells.

Furthermore, endogenous δ-SG at the sarcolemma (SL) might be reliable for identifying the engrafted skMb and its maturation, because of the three reasons listed below; (1) δ-SG exclusively exists in muscle cells, but not in other contaminant cells [22,23], (2) Among all SGs, δ-SG is exceptionally expressed throughout myogenesis from myoblast to myocyte [24] and (3) δ-SG is the most resistant to hydrolysis by an endogenous protease, m-calpain, which degrades other SGs as well as dystrophin *in vitro* [10]. Unique characters of m-calpain are compatible with recent scheme that the loss of component of SG proteins may be caused by the activated m-calpain secondary to pathogenic conditions [11,12,23,25]. All of these settings are associated with the disruption of dystrophin and increment of the SL permeability, resulting in the vicious cycle of cardiac muscle degeneration in failing hearts in various animal models and humans [9].

Time-dependent expression of fast- and slow-twitch MHCs in DCM heart

Preliminary study with skin grafting indicated an immunological tolerance between the control and TO-2 strain hamsters (Tezuka et al., in press). At 5 weeks after the skMb transplantation, double fluorescence microscopy revealed that ~90% of the engrafted cells identified by δ-SG expression on the SL (Fig. 1A) coexhibited prelabeled $DAPI^+$ nuclei beneath the SL (pink arrows in Fig. 1B) or at the center of myoplasm (pink arrowheads in Fig. 1B). They showed an alternative staining for fast-twitch MHC (red arrowheads in Fig. 1C) or slow-twitch MHC (blue arrows in Fig. 1D) in the adjacent serial sections. Because amino acid sequence of slow-twitch MHC is the same as β cardiac MHC (26), immunological identification using MHC antibodies was difficult to discriminate transfected slow-muscle fibers from the recipient cardiomyocytes.

We employed another marker, δ-SGs as donor-derived cells. Those cells presenting fast- twitch isoform of MHC were more abundant than those presenting slow-twitch MHC (blue arrows in Fig. 1D). Some cells (~10%) were stained for both the slow and fast isoforms of MHC (yellow arrows in Figs. 1C, D). Quadriceps femoris muscle from which the skMb allografts were prepared showed δ-SG on the SL (data not shown) and demonstrated an alternative expression of fast- or slow- twitch MHC. No cells were co-stained with both fast- and slow-twitch MHC antibodies. The predominant expression of fast-twitch MHC after the engraftment was similar to original constituent of MHC isoform in normal donor muscle.

At 15 weeks, the population of fast- and slow-twitch MHC^+ cells was reversed. Most cells (~80%) that were intensely stained with anti-δ-SG antibody (yellow arrows in Fig. 1E) or weakly stained (yellow arrowheads in Fig. 1E) matched with pre-labeled $DAPI^+$ nuclei of the engrafted cells beneath the SL (pink arrows in Fig. 1F) or at the center of myoplasm (pink arrowheads in Fig. 1F). The cells with an intense staining for δ-SG (yellow arrowheads in Fig. 1E) expressed slow- twitch MHC (blue arrows in Fig. 1H) and the rest shrunk cells with a weak stain for δ-SG (yellow arrowheads in Fig. 1E) revealed co-expression of both fast- and slow MHCs (blue arrowheads in Fig. 1G, Fig. 2H). The cells exclusively demonstrating fast-twitch MHC were not detected.

Please cite this article in press as: A. Tezuka et al., Which skeletal myoblasts and how to be transplanted for cardiac repair?, Biochem. Biophys. Res. Commun. (2008), doi:10.1016/j.bbrc.2007.11.084

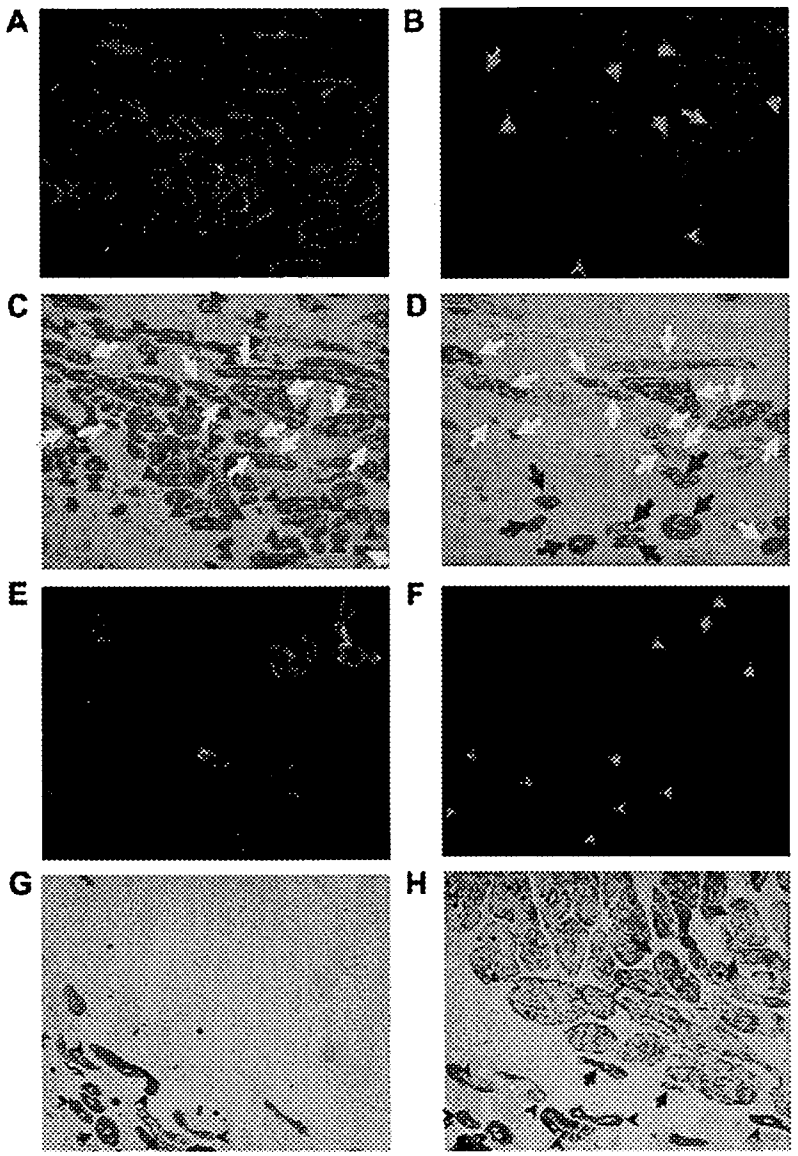

Fig. 1. Histological evaluation of engrafted skMbs in TO-2 heart at 5 weeks (A–D) or 15 weeks (E–H) after the cell transplantation. Double fluorescence microscopy of FITC-labeled antibody to δ-SG (A) or DAPI-prelabeled nuclei (B) of the donor cells shows the predominant expression of fast-twitch MHC (orange arrowheads in C, G), compared with slow-twitch MHC (D,H). Note that some cells expressed both fast-twitch and slow-twitch MHC (yellow arrows in C and D). Nuclei of engrafted skMbs with intense staining along SL (yellow arrows in E) and weak staining (yellow arrowheads in E) were situated at the center (pink arrows in F) and the subsarcolemma (pink arrowheads in F) of engrafted cells, respectively. Blue arrows and arrowheads in G or H denote the engrafted skMbs expressing slow-twitch MHC alone and both fast- and slow-twitch MHC, respectively. Original magnification 100×, and bar length indicates 100 μm.

The fast-twitch MHC in δ-SG$^+$ cells occupied 66.0 ± 7.1% at 5 weeks and decreased to 1.3 ± 1.0% at 15 weeks (Fig. 2A, $p < 0.01$). In contrast, the expression level of the slow-twitch MHC shared 23.0 ± 1.1% of δ-SG$^+$ cells at 5 weeks and enhanced to 80.0 ± 9.0% at 15 weeks ($p < 0.01$). Within 10-week interval, the estimated cell number of fast-MHC$^+$ cells drastically reduced in the whole heart (Fig. 2B), while Cx-43$^+$ cells slightly but significantly increased ($p < 0.05$). It should be intensified that the number of slow-twitch MHC$^+$/δ-SG$^+$ cells remained unchanged between 5 and 15 weeks after the cell transplantation ($27.3 \pm 9.7 \times 10^3$ *vs.* $18.2 \pm 5.0 \times 10^3$, respectively).

The time-dependency of cell population was confirmed by the Western blotting of fast-twitch MHC protein. Compared with the trace expression in cultured skMbs (Fig. 2C, lane s), the protein density corresponding to the fast-twitch MHC increased 5.99 ± 1.58-fold (Fig. 2C, lanes a–d, $n = 4$) at 5 weeks after the cell transplantation, suggesting the differentiation from skMbs to matured fast-twitch myocytes and their proliferation in the host hearts. Considering the total amount of protein in whole left ventricular muscle and skMbs, enormous amount of fast-twitch MHC was estimated to be synthesized after the cell-transplantation.

Please cite this article in press as: A. Tezuka et al., Which skeletal myoblasts and how to be transplanted for cardiac repair?, Biochem. Biophys. Res. Commun. (2008), doi:10.1016/j.bbrc.2007.11.084

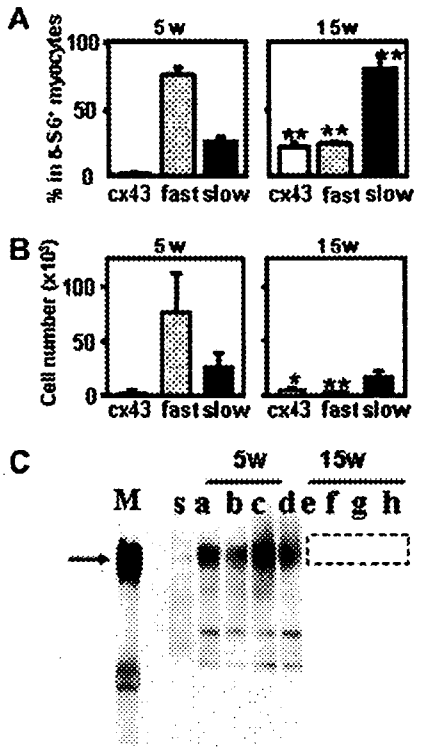

Fig. 2. Time-dependent alteration of positive cell-rates for Cx-43, fast- or slow-twitch MHC in δ-SG$^+$ cells at 5 and 15 weeks after the skMb-transplantation (A) or estimated cell-number in whole heart (B). Western blotting of fast-twitch MHC (arrow in upper picture) in the hearts of TO-2 hamsters at 5 (a–d) or 15 weeks (e–h) after the skMb-transplantation (C). M, T, and s denote the positive control of fast-twitch MHC, TO-2 heart without the cell-transplantation, and whole protein sample in skMbs applied, respectively. Note the huge production of fast-twitch MHC at 5 weeks, but the trace expression at 15 weeks (within a rectangle under lane e–h).

At 15 weeks after the cell transplantation, however, the amount of fast-twitch MHC dramatically reduced (0.36 ± 0.04-fold, $p < 0.01$), suggesting the trace expression (Fig. 2C, within a dotted rectangle in lanes e–h, $n = 4$). The interval between 5 and 15 weeks in hamsters corresponded to ~12 years in humans, as it would be sufficiently long to evaluate therapeutic efficacy of the cell transplantation.

Morphological alterations of engrafted myoblasts

The connexin (Cx)-43 expression in facet between the grafted and host cells was also dependent on the duration after the engraftment. At 5 weeks after the cell-transplantation, most of engrafted cells did not show Cx-43 between the donor and the host cells (data not shown). At 15 weeks after, however, more than 10% of the transplanted cells carrying δ-SG demonstrated positive staining for Cx-43 (Figs. 3A and B), suggesting that Cx-43 synthesized *de novo* in the engrafted cells formed a gap junction (Figs. 3B and F) and might serve for an electrical conduction, as is the case between cardiac muscle cells [21]. Double fluorescence microscopy of δ-SG immunostaining and Dil as the SL marker to identify the donor cells clearly demonstrated that not all transplanted skMbs, but the δ-SG$^+$ and Dil$^+$ cells, selectively presented Cx-43 (Fig. 3C). Between 5 and 15 weeks after the cell-transplantation, the cell population co-expressing both Cx-43 and δ-SG on the same cells increased 4-fold (from $2.56 \pm 0.55\%$ to $10.4 \pm 3.7\%$, $p < 0.01$, Fig. 2A).

Furthermore, serial adjacent sections (Figs. 3D–F) using triple or quadra-staining with Dil (red), DAPI (blue), δ-SG (green), and fast-twitch (Fig. 3D) or slow-twitch MHC (Fig. 3E) distinctly indicated that the engrafted skMbs present cardiac muscle-like features at 15 weeks after the cell- engrafting for the following four reasons; (1) the expression of Cx-43 specific to myocardial cell (Figs. 3A and B), (2) selective production of not fast-twitch (Fig. 3D), but slow-twitch MHC (Fig. 3E) of which the amino acid sequence completely matched with cardiac MHC [26], and (3) single nucleus at the center of myoplasm of the engrafted cells like cardiomyocytes (pink arrow in Fig. 3F), being totally different from skeletal muscle cells that show multiple nuclei beneath the SL.

Cell density-dependent degeneration of grafted skMbs

The survival of engrafted cells was dependent on the cell density for the transplantation. In sham operation without the cell-transplantation, no cells showed Dil (Fig. 4A) in TO-2 heart and numerous TUNEL$^+$ nuclei (Fig. 4B) at the locus corresponding to the degraded tissue (Fig. 4C). When skMbs were transplanted at the locally dense condition (Fig. 4D), TUNEL$^+$ cells became scarcely detected except the non-specific staining at the site corresponding to the densely located Dil$^+$ cells (Fig. 4E) and degraded myocardium (Fig. 4F).

In contrast, when prelabeled Dil$^+$ skMbs were sparsely disseminated in TO-2 heart (Fig. 4G), no cells demonstrated TUNEL$^+$ staining (Fig. 4H) and showed neatly arranged myocardium without degradation (Fig. 4I). In the progression of heart failure from mild to advanced stage, not only apoptosis but also autophagy would contribute to myocardial cell death in DCM hearts [27]. Because TUNEL staining uses end-labeling of fragmented DNA, it was difficult to precisely discriminate these two types of cell-death. Present results, however, clearly demonstrate that sparse and diffuse delivery was preferable for the efficient cell-engrafting.

The exact reason why not all DiI$^+$ cells present δ-SG was unclear (Fig. 3C). It would be conceivable that fast-twitch myocytes with highly energy-consuming and requiring large amount of oxygen and nutrients might be eradicated by the natural selection secondary to apoptosis (Fig. 4E) in TO-2 heart, leaving slow-twitch muscles under the limited myocardial slow. In general, the amount of constituent protein is dependent on the dynamic equilibrium of biosynthesis and the proteolysis *in vivo*. We have shown that dystrophin and its related proteins remained constant at the early phase of ischemic cardiomyopathy without

Please cite this article in press as: A. Tezuka et al., Which skeletal myoblasts and how to be transplanted for cardiac repair?, Biochem. Biophys. Res. Commun. (2008), doi:10.1016/j.bbrc.2007.11.084

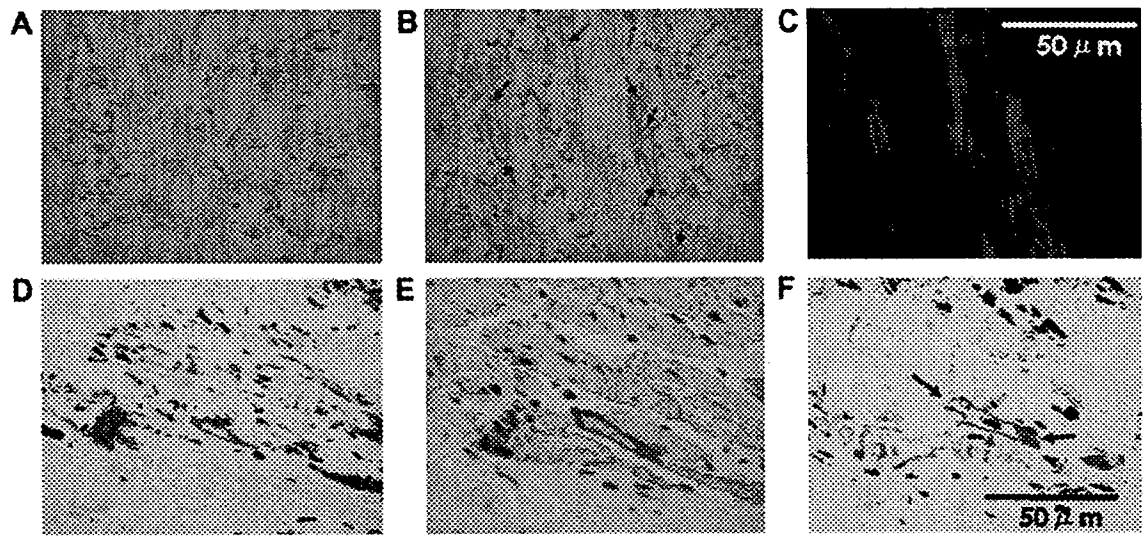

Fig. 3. Connexin (Cx)-43 expression between the engrafted skMbs and host cardiomyocytes. Immunostaining of Cx-43 (A), merged picture with δ-SG along SL (B), and double fluorescence picture of δ-SG and DiI-prelabeled skMbs (C). Quadra-staining of serial three sections of engrafted cells in TO-2 heart at 15 weeks (D–F). Red, blue, and green indicate florescence of DiI for the SL, DAPI for the nucleus, and FITC-labeled antibody to δ-SG, respectively. Note that the engrafted skMbs expressed δ-SG along the SL (D–F), not fast-twitch (D), but slow-twitch MHC (E), Cx-43 at both ends (black arrows in F), and nucleus at the center of the myoplasm (pink dashed arrow in F). Original magnification 100×, and bar length indicates 100 μm.

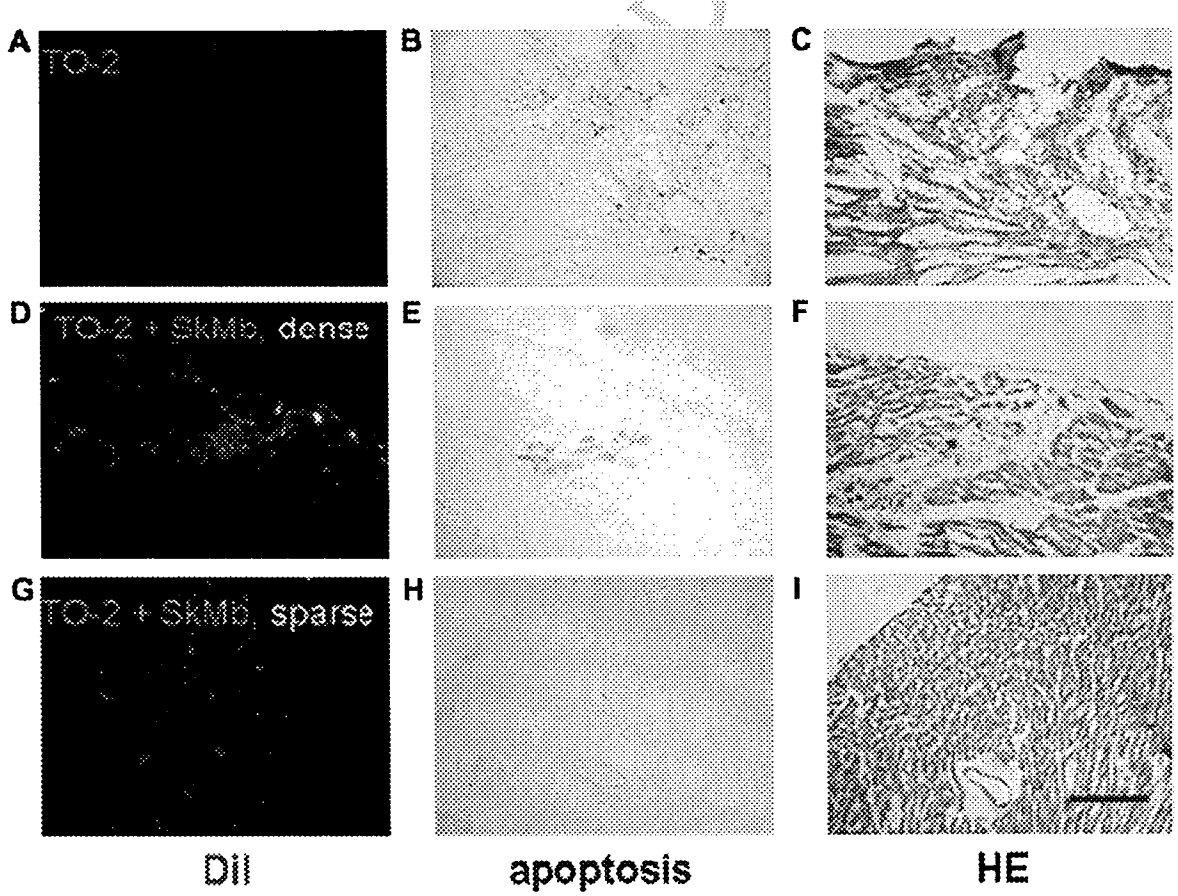

Fig. 4. Cell density dependent apoptosis and/or autophagy of engrafted cells detected by TUNEL staining in TO-2 hearts. Without cell-transplantation, most cells showed no DiI (A) and numerous TUNEL$^+$ nuclei (B) at the loci corresponding to degraded myocardium (HE staining in C). When the skMbs were transplanted at locally dense condition (upper DiI$^+$ portion near to epicardium, D), TUNEL$^+$ cells were scarcely detected except the non-specific staining at the densely transplanted site (E) and degraded myocardium (F). In contrast, when DiI$^+$ skMbs were sparsely disseminated in TO-2 heart (G), no cells showed TUNEL$^+$ staining (H) in neatly arranged myocardium (I). Original magnification 100×, and bar length indicates 100 μm.

Please cite this article in press as: A. Tezuka et al., Which skeletal myoblasts and how to be transplanted for cardiac repair?, Biochem. Biophys. Res. Commun. (2008), doi:10.1016/j.bbrc.2007.11.084

heart failure, accompanying the compensatory overexpression of each mRNA. In contrast, at the end stage of heart failure, no compensatory expression of both the transcript and transgene caused loss of these proteins, being exceeded by their increased proteolysis [11]. The cell subgroup with less intense δ-SG$^+$ at 15 weeks after the skMb-transplantation (Fig. 2A) might represent the degrading cells during the selection of transplanted cells.

Pouly et al. have reported functional efficacy of skeletal myoblast transplantation, using CHF147 strain hamsters which genetically lack δ-SG gene [28]. At 4 weeks after the intramural administration of skMb, 2D echo study revealed functional improvement, myotube formation, and positive staining for fast-twitch MHC of skeletal muscle cells. The histological study also demonstrated multinuclear fiber oriented parallel to the surrounding cardiac cells. These findings are in agreement with our data at 5 weeks in TO-2 strain after the cell-transplantation, though the expression of slow-twitch MHC was not examined. As was shown by Attar et al. [29], long-term follow-up to 1 year in rat myocardial infarction model demonstrated the functional benefits of autologous skMb transplantation. However, they reported that both the fast- and slow-twitch MHC isoforms were expressed. The exact reason of discrepancy is unknown, but might caused by the difference between the clinical stetting *i.e.*, DCM of genetic origin and myocardial infarction.

Effect of skMb-transplantation on hemodynamics and arrhythmia

When hemodynamic study was restricted to the disseminated engrafted cases ($n = 6$) in the autopsy, the skMb transplantation on the hemodynamics was shown to be beneficial for improving several indices. The available space to discuss the effect on physiological action is limited and will be presented in the supplementary section.

Current results would imply the therapeutic significance in cell-transplantation employing not the mixture of fast- and slow-twitch cells that may cause either substrate for serious arrhythmias or heterogeneous contraction, but selected slow-twitch muscle cells carrying the similar characteristics as cardiac muscle fibers with enduring mechanical performance, metabolic activities [30] as well as homogeneous electric conduction *via* Cx-43 and intercalated disc synthesized *de novo*. Future cardiac repair for the regenerative medicine should target the progenitor cells with similar properties to cardiac muscle cells and how to select the slow-twitch myoblasts *ex vivo*.

Appendix A. Supplementary data

Supplementary data associated with this article can be found, in the online version, at doi:10.1016/j.bbrc.2007.11.084.

References

[1] J.M. Leiden, The genetics of dilated cardiomyopathy-Emerging clues to the puzzle, N Engl. J. Med. 337 (1997) 1080–1081.
[2] D.A. Taylor, B.Z. Atkins, P. Hungspreugs, et al., Regenerating functional myocardium: improved performance after skeletal myoblast transplantation, Nat. Med. 4 (1998) 929–933.
[3] P. Menasche, A.A. Hagège, M. Scorsin, et al., Myoblast transplantation for heart failure, Lancet 357 (2001) 279–280.
[4] A.A. Hagège, C. Carrion, P. Menasche, et al., Viability and differentiation of autologous skeletal myoblast grafts in ischaemic cardiomyopathy, Lancet 361 (2003) 491–492.
[5] P. Menasche, A.A. Hagège, J.T. Vilquin, et al., Autologous skeletal myoblast transplantation for severe postinfarction left ventricular dysfunction, J. Am. Coll. Cardiol. 41 (2003) 1078–1083.
[6] P.C. Smits, R.J. van Geuns, D. Poldermans, et al., Catheter-based intramyocardial injection of autologous skeletal myoblasts as a primary treatment of ischemic heart failure: clinical experience with six-month follow-up, J. Am. Coll. Cardiol. 42 (2003) 2063–2069.
[7] P. Menasche, First randomized placebo-controlled myoblast autologous grafting in ischemic cardiomyopathy (MAGIC) trial. AHA scientific meetings late-breaking clinical trial session, Chicago, November 15, 2006.
[8] T. Kawada, M. Nakazawa, S. Nakauchi, et al., Rescue of hereditary form of dilated cardimyopathy by rAAV-mediated somatic gene therapy: amelioration of morphological findings, sarcolemma permeability, cardiac performances, and the prognosis of TO-2 hamsters, Proc. Natl. Acad. Sci. USA 99 (2002) 901–906.
[9] T. Toyo-oka, T. Kawada, J. Nakata, et al., Translocation and cleavage of myocardial dystrophin as a common pathway to advanced heart failure, Proc Natl. Acad. Sci. USA 101 (2004) 7381–7385.
[10] H. Yoshida, M. Takahashi, M. Koshimizu, et al., Decrease in sarcoglycans and dystrophin in failing heart following acute myocardial infarction, Cardiovasc. Res. 59 (2003) 419–427.
[11] M. Takahashi, K. Tanonaka, H. Yoshida, et al., Effects of ACE inhibitor and AT_1 blocker on dystrophin-related proteins and calpain in failing heart, Cardiovasc. Res. 65 (2005) 356–365.
[12] A. Sakamoto, K. Ono, M. Abe, et al., Both hypertrophic and dilated cardiomyopathies are caused by mutation of the same gene, δ-sarcoglycan, in hamster, Proc. Natl. Acad. Sci. USA 94 (1997) 13873–13878.
[13] V. Nigro, Y. Okazaki, A. Belsito, et al., Identification of the Syrian hamster cardiomyopathy gene, Hum. Mol. Genet. 6 (1997) 601–607.
[14] S. Tsubata, K.R. Bowles, M. Vatta, et al., Mutations in the human δ-sarcoglycan gene in familial and sporadic dilated cardiomyopathy, J. Clin. Invest. 106 (2000) 655–662.
[15] K.A. Lapidos, Y.E. Chen, J.U. Earley, et al., Transplanted hematopoietic stem cells demonstrate impaired sarcoglycan expression after engraftment into cardiac and skeletal muscle, J. Clin. Invest. 114 (2004) 1577–1585.
[16] M.S. Parmacek, J.A. Epstein, Pursuing cardiac progenitors: regeneration redux, Cell 120 (2005) 295–298.
[17] H. Reinecke, V. Poppa, C.E. Murray, Skeletal muscle stem cells do not transdiffentiate into car diocytes after cardiac grafting, J. Mol. Cell. Cardiol. 34 (2002) 241–249.
[18] A. Rosenzweig, Cardiac cell therapy-Mixed results from mixed cells, N. Engl. J. Med. 355 (2006) 1274–1277.
[19] K. Lunde, S. Solheim, S. Aakhus, et al., Intracoronary injection of mononuclear bone marrow cells in acute myocardial infarction, N. Engl. J. Med. 355 (2006) 1199–1209.
[20] V. Schachinger, S. Erbs, A. Elsasser, et al., Intracoronary bone marrow-derived progenitor cells in acute myocardial infarction, N. Engl. J. Med. 355 (2006) 1210–1221.
[21] B. Assmus, J. Honold, V. Schachinger, et al., Transcoronary transplantation of progenitor cells after myocardial infarction, N. Engl. J. Med. 55 (2006) 1222–1232.

Please cite this article in press as: A. Tezuka et al., Which skeletal myoblasts and how to be transplanted for cardiac repair?, Biochem. Biophys. Res. Commun. (2008), doi:10.1016/j.bbrc.2007.11.084

[22] K.P. Campbell, Three muscular dystrophies: loss of cytoskeleton-extracellular matrix linkage, Cell 80 (1995) 675–679.
[23] T. Kawada, F. Masui, A. Tezuka, et al., A novel scheme of dystrophin disruption for the prgression of advanced heart failure. A review, Biochim. Biophys. Acta 1751 (2005) 73–81.
[24] L.A. Liu, E. Engvall, Sarcoglycan isoforms in skeletal muscle, J. Biol. Chem. 274 (1999) 38171–38175.
[25] H. Xi, W.S. Shin, J. Suzuki, et al., Dystrophin disruption might be related to myocardial cell apoptosis caused by isoproterenol, J. Cardiovasc. Pharmacol. 36 (Suppl. 2) (2000) S25–S29.
[26] K. Yamauchi-Takihara, M.J. Sole, J. Liew, et al., Characterization of human cardiac myosin heavy chain genes, Proc. Natl. Acad. Sci. USA 86 (1989) 3504–3508.
[27] S. Miyata, G. Takemura, Y. Kawase, et al., Autophagic cardiomyocyte death in cardiomyopathic hamsters and its prevention by granulocyte colony-stimulating factor, Am. J. Pathol. 168 (2006) 386–397.
[28] J. Pouly, A.A. Hagège, J.T. Vilquin, et al., Does the functional efficacy of skeletal myoblast transplantation extend to nonischemic cardiomyopathy? Circulation 110 (2004) 1626–1631.
[29] N.A. Attar, C. Carrion, S. Ghostine, et al., Long-term functional and histological results of autologous skeletal muscle cells transplantation in rat, Cardiovasc. Res. 58 (2003) 142–148.
[30] C.J. Barclay, Mechanical efficiency and fatigue of fast and slow muscles of the mouse, J. Physiol. 497 (1996) 781–794.

Please cite this article in press as: A. Tezuka et al., Which skeletal myoblasts and how to be transplanted for cardiac repair?, Biochem. Biophys. Res. Commun. (2008), doi:10.1016/j.bbrc.2007.11.084

Usefulness of the brain natriuretic peptide to atrial natriuretic peptide ratio in determining the severity of mitral regurgitation

Ken Shimamoto MD, Miyako Kusumoto MD, Rieko Sakai MD, Hirota Watanabe MD, Syunichi Ihara MD, Natsuha Koike MD, Masatoshi Kawana MD

K Shimamoto, M Kusumoto, R Sakai, et al. Usefulness of the brain natriuretic peptide to atrial natriuretic peptide ratio in determining the severity of mitral regurgitation. Can J Cardiol 2007;23(4):295-300.

BACKGROUND: Atrial natriuretic peptide (ANP) and brain natriuretic peptide (BNP) levels were characterized in subjects with mitral regurgitation (MR).

METHODS: Sixty-two cases of moderate or severe chronic MR were studied. The blood levels of neurohormonal factors were stratified by the known MR prognostic factors of New York Heart Association (NYHA) functional class, left ventricular end-diastolic diameters, left ventricular end-systolic diameter (LVDs), ejection fraction (EF), left atrial diameter and presence of atrial fibrillation (AF).

RESULTS: ANP levels were higher in NYHA class II and lower in classes I and III/IV (P=0.0206). BNP levels were higher in NYHA class II than class I (P=0.0355). The BNP/ANP ratio was significantly higher in NYHA classes II and III/IV than in class I (P=0.0007). To differentiate between NYHA classes I/II and III/IV, a cut-off BNP/ANP ratio of 2.97 produced a sensitivity of 78% and specificity of 87%. Compared with subjects in sinus rhythm, patients with AF had an enlarged left atrium and lower ANP levels. The BNP/ANP ratio correlated significantly with left atrial diameter, LVDs and EF (r=0.429, P=0.0017; r=0.351, P=0.0117; and r=–0.349, P=0.0122; respectively), and was significantly higher among all the known operative indications for MR tested (LVDs 45 mm or more, EF 60% or less, NYHA class II or greater and AF; P=0.0073, P=0.003, P=0.0102 and P=0.0149, respectively).

CONCLUSIONS: In chronic MR, levels of ANP and BNP, and the BNP/ANP ratio are potential indicators of disease severity.

Key Words: *Atrial natriuretic peptide; Brain natriuretic peptide; Cardiac function; Heart failure; Mitral regurgitation*

L'utilité du ratio entre le peptide natriurétique cérébral et le peptide natriurétique auriculaire pour déterminer la gravité de la régurgitation mitrale

HISTORIQUE : Les taux de peptide natriurétique auriculaire (PNA) et de peptide natriurétique cérébral (PNC) étaient caractéristiques chez des sujets atteints de régurgitation mitrale (RM).

MÉTHODOLOGIE : On a étudié 62 cas de RG chronique modérée à grave. On a stratifié les taux sanguins de facteurs neuro-hormonaux selon les facteurs pronostiques connus de RM pour la classe fonctionnelle de la *New York Heart Association* (NYHA), les diamètres ventriculaires gauches en fin de diastole, le diamètre ventriculaire gauche en fin de systole (DVG), la fraction d'éjection (FE), le diamètre auriculaire gauche et la présence de fibrillation auriculaire (FA).

RÉSULTATS : Les taux de PNA étaient plus élevés dans la classe II de la NYHA et plus faibles dans les classes I et III/IV (P=0,0206). Les taux de PNC étaient plus élevés dans la classe II de la NYHA que dans la classe I (p = 0,0355). Le ratio PNA/PNC était considérablement plus élevé dans les classes II et III/IV de la NYHA que dans la classe I (P=0,0007). Pour distinguer la classe I/II de la NYHA de la classe III/IV, un ratio PNA/PNC seuil de 2,97 produisait une sensibilité de 78 % et une spécificité de 87 %. Par rapport aux sujets ayant un rythme sinusal, les patients atteints de FA présentaient une hypertrophie auriculaire gauche et des taux de PNA plus faibles. Le ratio PNA/PNC était corrélé de manière significative avec le diamètre auriculaire gauche, les DVG et la FE (r = 0,429, p = 0,0017; r = 0,351, p = 0,0117; et r = –0,349, p = 0,0122; respectivement) et était considérablement plus élevé dans toutes les indications connues de RM évaluées (DVG 45 mm ou plus, FE 60 % ou moins, classe II de la NYHA ou plus et FA; p = 0,0073, p = 0,003, p = 0,0102 et p = 0,0149, respectivement).

CONCLUSIONS : En cas de RM chronique, les taux de PNA et de PNC et le ratio PNA/PNC sont des indicateurs potentiels de la gravité de la maladie.

In chronic mitral regurgitation (MR), increased preload and reduced afterload due to unloading from the left ventricle (LV) into the left atrium (LA) leads to compensatory dilation of the LV and facilitates LV ejection. Although this response initially maintains cardiac output, myocardial decompensation eventually results in heart failure symptoms and an increased risk of sudden death. In addition, backflow into the LA results in enlargement of the LA, atrial fibrillation and elevated pulmonary pressures. In some patients, LV contractility is irreversibly impaired in the absence of symptoms (1-3). Thus, deferring surgical intervention often leads to irreversible postoperative LV dysfunction. Valve replacement or valvuloplasty is essential before the myocardial damage becomes irreversible. Early valvuloplasty conducted when heart failure is mild has been reported to improve prognosis (4). In clinical practice, however, it remains difficult to decide the timing of surgery defined by mild heart failure symptoms and preserved cardiac function.

Some reports have shown that preoperative LV function (LV end-diastolic diameter [LVDd], LV end-systolic diameter [LVDs] and ejection fraction [EF]), LV wall thickness, LA size, LA area, pulmonary hypertension, and atrial fibrillation are good predictors of survival and postoperative LV dysfunction. The American College of Cardiology/American Heart Association guidelines recommend considering symptoms and LV function, especially EF and LVDs, as useful parameters in

Department of Cardiology, Tokyo Women's Medical University, Aoyama Hospital, Tokyo, Japan
Correspondence and reprints: Dr Masatosho Kawana, Department Cardiology, Tokyo Women's Medical University, Aoyama Hospital, 2-7-13 Kita Aoyama, Minato-ku, Tokyo 107-0061, Japan. Telephone 81-3-5411-8111, fax 81-3-5411-8126, e-mail mkawana@hij.twmu.ac.jp
Received for publication January 3, 2006. Accepted July 16, 2006

TABLE 1
Baseline characteristics of patients grouped according to functional severity

Variable	Overall (n=62)	NYHA class I (n=8)	NYHA class II (n=35)	NYHA class III/IV (n=19)	P (by ANOVA or χ^2)
Age, years (mean ± SD)	63.6±13.2	54.7±16.4	64.6±13.1	65.3±11.4	0.1582
Male sex, %	76				
Prolapse/torn chordae tendineae, n	62/3				
Systolic BP, mmHg (mean ± SD)	123.6±20.8	122.3±14.6	124.6±20.0	121.7±22.8	0.9019
Diastolic BP, mmHg (mean ± SD)	69.9±12.9	70.3±7.3	69.1±11.0	71.7±19.0	0.8474
Heart rate, beats/min (mean ± SD)	71.9±12.8	67.8±11.7	70.9±11.9	76.3±15.1	0.3497
Serum creatinine, μmol/L (mean ± SD)	97.2±35.4	79.6±26.5	88.4±17.7	132.6±44.2*†	0.0043
Serum sodium, mmol/L (mean ± SD)	140.2±2.5	140.6±2.2	140.2±2.8	140.1±2.2	0.0810
Serum potassium, mmol/L (mean ± SD)	4.0±0.4	3.9±0.3	4.1±0.4	4.0±0.5	0.8372
Atrial fibrillation, n	37	1	20	16	0.0022‡
Concomitant drugs, n					
Digitalis		2	19	8	0.2889‡
Furosemide		0	20	19	0.0068‡
Spironolactone		0	13	6	0.1202‡
Angiotensin-converting enzyme inhibitors		3	13	10	0.9126‡
Angiotensin receptor blockers		0	2	3	0.2877‡
Nitrates		0	13	9	0.0604‡
Calcium antagonists		2	7	2	0.5802‡

P<0.05 versus New York Heart Association (NYHA) class I, Tukey-Kramer's post hoc test; †P<0.05 versus NYHA class II, Tukey-Kramer's post hoc test. ‡Goodness-of-fit test for χ^2. BP Blood pressure

clinical decision making on the timing of an operation (2). However, little data are available on the association of neurohormonal factors with operative indication. With the above background, we evaluated whether atrial natriuretic peptide (ANP) and brain natriuretic peptide (BNP) levels may indicate the severity of MR and timing of surgery by comparison with the known prognostic factors and operative indications.

METHODS

Sixty-two cases of chronic MR with at least moderate regurgitation on echocardiography or at least Sellar class 3 regurgitation on LV angiography diagnosed in the Department of Cardiology at the Aoyama Hospital (Tokyo, Japan) between 1996 and 2002 were studied. The cases included 47 men and 15 women with a mean (± SD) age of 63.6±13.2 years (range 31 to 85 years). Patients with acute heart failure and acute exacerbations of chronic heart failure were excluded. MR was caused by prolapse in all 62 cases and by torn chordae tendineae in three cases, as revealed by echocardiography. Seven patients had a history of hypertension, four patients had diabetes and one patient had cerebrovascular disease. The degree of heart failure according to the New York Heart Association (NYHA) functional classification was class I in eight cases, class II in 35 cases, class III in 14 cases and class IV in five cases. The medical therapy, clinical findings and biochemical profiles by NYHA class are shown in Table 1.

At the hospital, all patients were treated with maximal medical treatment using diuretics and vasodilators. After patients were stabilized, blood was collected in the early morning, with the patients at rest for radioimmunoassay measurements of the ANP, BNP and serum norepinephrine levels, plasma renin activity and plasma aldosterone concentration. Cardiac function was evaluated by echocardiography, and LA diameter (LAd), LVDd, LVDs, EF and right ventricular systolic pressure (RVSP) were measured. In five NYHA class I cases, tricuspid regurgitation was not detected, and RVSP could not be measured. Operative criteria for MR were determined in accordance with the American College of Cardiology/American Heart Association guidelines (2).

Echocardiographic methods

All subjects underwent standard two-dimensional echocardiography with a commercially available system (Hewlett Packard Sonos 5500, Hewlett Packard, USA) using a multifrequency MHz transducer. LV and LA dimensions were obtained by M-mode echocardiography, guided by two-dimensional imaging. Mitral valve prolapse was defined as the superior displacement of the leaflets during systole in a two-dimensional echocardiographic long-axis view of the LV. The degree of MR was assessed by the size, penetration and flow velocity of the regurgitant jet (5).

Measurement of natriuretic peptide levels

Once patients had been in a supine position for at least 60 min after waking, a blood sample drawn from a peripheral vein was immediately placed on ice and transferred to the laboratory at the same hospital. After plasma extraction, the samples were stored in a deep freezer until they were used. BNP and ANP levels were measured by standard radioimmunoassay (Shionoria ANP kit and Shionoria BNP kit, Shionogi & Co, Japan) within 24 h. The normal values of ANP and BNP are less than 13.9 pmol/L (43 pg/mL), and less than 5.3 pmol/L (18.4 pg/mL), respectively.

Statistical analysis

Continuous variables are expressed as mean ± SD, unless otherwise stated. Differences between groups described by categorical variables were analyzed by the χ^2 test for goodness-of-fit. Simple linear regression analyses were performed to correlate neurohormonal levels with echocardiographic parameters and NYHA functional class. Clinical variables and NYHA class were assessed by ANOVA, followed by Tukey-Kramer's post hoc test, as appropriate. For the relationship between neurohormonal levels and operative criteria, a Mann-Whitney's U test was performed. All P<0.05 were regarded

TABLE 2
Clinical results of patients grouped according to functional severity

Variable	NYHA class I (n=8)	NYHA class II (n=35)	NYHA class III/IV (n=19)	P (by ANOVA)
Echocardiography (mean ± SD)				
LVDd, mm	60.6±6.8	59.7±6.7	66.7±11.2†	0.0232
LVDs, mm	36.4±5.7	37.6±7.0	46.4±8.8*†	0.0004
EF, %	64.8±7.0	61.0±9.1	51.7±9.5*†	0.0007
LAd, mm	41.1±1.6	49.5±9.0	64.2±12.3*†	<0.0001
RVSP, mmHg	33.1±3.6	51.8±16.2	52.8±14.1	0.1180
Neurohormones (mean ± SD)				
PRA, ng/L/s	1.2±1.3	1.3±1.3	1.5±1.0	0.7318
PAC, nmol/L	0.24±0.09	0.35±0.32	0.28±0.24	0.5996
sNA, pmol/L	1243.2±355.2	2545.6±1065.6	3078.4±1953.6	0.0796
ANP, pmol/L	8.4±10.7	35.9±36.9	16.3±15.4	0.0206
BNP, pmol/L	7.7±11.6	62.1±56.0*	56.6±43.9	0.0355

*Clinical variables and New York Heart Association (NYHA) class were assessed by ANOVA, and then Tukey-Kramer's post hoc test, as appropriate. *P<0.05 versus NYHA class I; †P<0.05 versus NYHA class II. ANP Atrial natriuretic peptide; BNP Brain natriuretic peptide; EF Ejection fraction; LAd Left atrial diameter; LVDd Left ventricular end-diastolic diameter; LVDs Left ventricular end-systolic diameter; PRA Plasma renin activity; PAC Plasma aldosterone concentration; RVSP Right ventricular systolic pressure; sNA Serum norepinephrine*

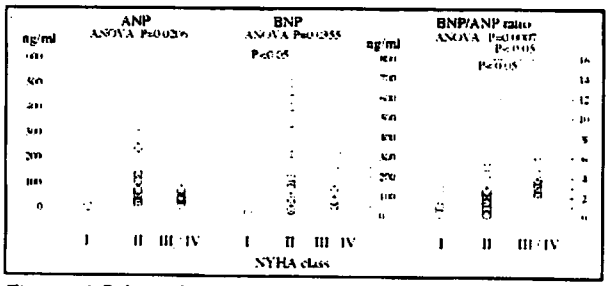

Figure 1) *Relationship of the New York Heart Association (NYHA) functional class with atrial natriuretic peptide (ANP) level, brain natriuretic peptide (BNP) level and the BNP/ANP ratio. No significant increases in ANP or BNP levels were observed in NYHA class III/IV. The BNP/ANP ratio increases with increased severity according to NYHA class*

as having statistical significance. To determine whether the BNP/ANP ratio predicts the severity of heart failure, the receiver-operating characteristic (ROC) curves for various cut-off BNP/ANP ratios were compared with NYHA class. Analyses were performed using StatView 5.0 software (SAS Institute, USA) and SPBS 9.37 software (ComWorks Co Ltd, Japan).

RESULTS

NYHA functional class and echocardiographic variables or neurohormonal plasma levels

As shown Table 2, the LVDd was significantly larger in class III/IV (ANOVA, P=0.0232; Tukey-Kramer's post hoc test, class II versus class III/IV, P<0.05) and LVDs was also significantly larger in class III/IV (ANOVA, P=0.0004; Tukey-Kramer's post hoc test, class I versus class III/IV, P<0.05; class II versus class III/IV, P<0.05). EF was significantly lower in NYHA class III/IV (ANOVA, P=0.0007; Tukey-Kramer's post hoc test, class I versus class III/IV, P<0.05; class II versus class III/IV, P<0.05). The LAd was significantly dilated in NYHA classes III/IV (ANOVA, P<0.0001; Tukey-Kramer's post hoc test, class I versus class III/IV, P<0.05; class II versus class III/IV, P<0.05). RVSP was not significantly different among the NYHA functional classes (ANOVA, P=0.1180).

There were no differences in plasma renin activity, plasma aldosterone concentrations or serum norepinephrine levels between patients in NYHA classes I, II and III/IV. The ANP level was significantly different among NYHA classes, showing a tendency to increase in class II and significantly decrease in classes III/IV (ANOVA, P=0.0206). The corresponding BNP level was higher in NYHA class II (ANOVA, P=0.0355; Tukey-Kramer's post hoc test, class I versus class II: P<0.05) (Table 2 and Figure 1).

TABLE 3
Correlation coefficients of neurohormones with cardiac function

Parameter			
Neurohormones	Cardiac function	r	P
PAC	Left atrial diameter	0.269	0.0742
	Left ventricular end-diastolic diameter	0.485	0.0008
	Left ventricular end-systolic diameter	0.361	0.0159
	Ejection fraction	−0.064	0.6801
PRA	Left atrial diameter	0.339	0.0227
	Left ventricular end-diastolic diameter	−0.056	0.7195
	Left ventricular end-systolic diameter	−0.054	0.7297
	Ejection fraction	0.023	0.8821
sNA	Left atrial diameter	0.475	0.0030
	Left ventricular end-diastolic diameter	0.461	0.0047
	Left ventricular end-systolic diameter	0.247	0.1465
	Ejection fraction	0.121	0.4812
ANP	Left atrial diameter	−0.179	0.1899
	Left ventricular end-diastolic diameter	−0.196	0.1546
	Left ventricular end-systolic diameter	−0.222	0.1063
	Ejection fraction	0.150	0.2802
BNP	Left atrial diameter	−0.038	0.7873
	Left ventricular end-diastolic diameter	−0.098	0.4838
	Left ventricular end-systolic diameter	−0.017	0.9038
	Ejection fraction	−0.095	0.4991
BNP/ANP ratio	Left atrial diameter	0.429	0.0017
	Left ventricular end-diastolic diameter	0.215	0.1300
	Left ventricular end-systolic diameter	0.351	0.0117
	Ejection fraction	−0.349	0.0122

ANP Atrial natriuretic peptide; BNP Brain natriuretic peptide; PAC Plasma aldosterone concentration; PRA Plasma renin activity; sNA Serum norepinephrine

Echocardiographic variables and neurohormonal plasma levels

A weak correlation was observed between plasma aldosterone concentration and LVDd (r=0.485, P=0.0008) or LVDs (r=0.361, P=0.0159), between plasma renin activity and LAd (r=0.339, P=0.0227), and between norepinephrine and LAd (r=0.475, P=0.003) or LVDd (r=0.461, P=0.0047). ANP and BNP levels showed no correlation with LAd, LVDd, LVDs and EF (Table 3).

LA size, atrial fibrillation and natriuretic peptides

Overall analysis showed no correlation between ANP levels and LAd (r=−0.073). While ANP levels increased with a mild increase in LAd, they decreased when the LAd was markedly

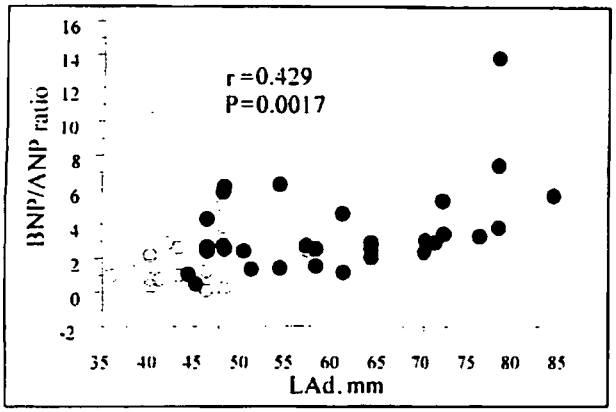

Figure 2) *Relationship of left atrial diameter (LAd) and brain natriuretic peptide (BNP) to atrial natriuretic peptide (ANP) ratio. The BNP/ANP ratio showed a positive correlation with LAd. Patients with atrial fibrillation (closed circles) had larger LAd than patients in sinus rhythm (open circles)*

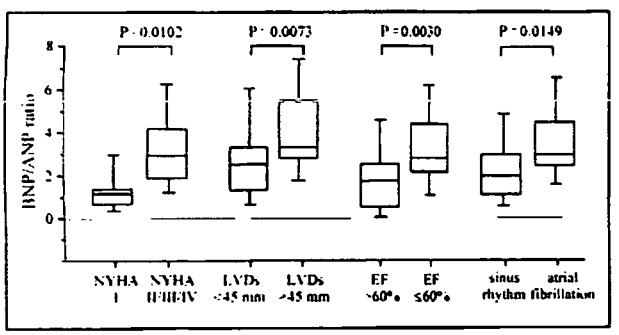

Figure 3) *Comparison of brain natriuretic peptide (BNP) to atrial natriuretic peptide (ANP) ratio by operative indications according to the American College of Cardiology/American Heart Association guidelines. Mann-Whitney's U test was performed. Box plot shows median (centre line), first and third quartiles (top and bottom of box), and lowest and highest values (vertical lines) of ANP and BNP level, and BNP/ANP ratio. Significant differences in BNP/ANP ratio were observed for all the American College of Cardiology/American Heart Association indications, comprising New York Heart Association (NYHA) functional class, left ventricular end-systolic diameter (LVDs), ejection fraction (EF) and presence of atrial fibrillation*

increased with increased atrial fibrillation. BNP levels showed the same tendency (Figure 2).

BNP/ANP ratio

The mean (± SD) BNP/ANP ratio (1.1±0.9 versus 2.4±1.9 versus 4.6±2.8 in NYHA classes I, II and III/IV, respectively) increased significantly in NYHA class III/IV (ANOVA, P=0.0007; Tukey-Kramer's post hoc test, class I versus classes III/IV, P<0.05; class II versus class III/IV, P<0.05) (Figure 1).

A weak correlation was detected between the BNP/ANP ratio and LVDs (r=0.351, P=0.0117) or EF (r=−0.349, P=0.0122) (Table 3). The BNP/ANP ratio increased with an increase in atrial diameter (r=0.429, P=0.0017) (Figure 2).

Operative indication and neurohormonal levels

The neurohormonal levels were compared between two groups divided by the known operative indications for MR, namely,

TABLE 4
Sensitivity and specificity of natriuretic peptide levels and echocardiographic parameters for symptoms

	NYHA class I versus class II/III/IV			NYHA class I/II versus class III/IV		
Variable	Sensitivity (%)	Specificity (%)	AUROC	Sensitivity (%)	Specificity (%)	AUROC
BNP	96	71	0.91	NA	NA	0.56
ANP	70	13	0.16	47	64	0.61
BNP/ANP	88	83	0.82	78	87	0.86
LAd	84	100	0.89	61	95	0.86
LVDs	38	100	0.66	39	100	0.79
EF	39	88	0.75	90	51	0.72

ANP Atrial natriuretic peptide; AUROC Area under the receiver-operating characteristic curve; BNP Brain natriuretic peptide; EF Ejection fraction; LAd Left atrial diameter; LVDs Left ventricular end-systolic diameter; NA Not available; NYHA New York Heart Association

NYHA class II or greater, EF 60% or less, LVDs 45 mm or larger and the presence of atrial fibrillation. No significant differences in plasma renin activity and plasma aldosterone concentration were observed for all the operative indications. The serum norepinephrine level was significantly higher in NYHA class II or greater (P=0.0083) and atrial fibrillation (P=0.0288). ANP level was significantly higher in NYHA class II or greater (P=0.0055), and BNP level was significantly higher in NYHA class II or greater (P=0.0006) and atrial fibrillation (P=0.0019). The BNP/ANP ratio was significantly higher in EF of 60% or less (P=0.0030), LVDs 45 mm or more (P=0.0073), NYHA class II or greater (P=0.0102) and the presence of atrial fibrillation (P=0.0149) (Figure 3).

ROC curves for NYHA classification

The clinical use of the BNP/ANP ratio as an indicator of disease severity was analyzed by ROC curves. The sensitivity, specificity and area under the ROC curve for symptoms by natriuretic peptide levels and echocardiographic measures are shown in Table 4. For NYHA classes II/III/IV, a cut-off BNP/ANP ratio of 1.20 produced a sensitivity of 88%, specificity of 83% and area under the ROC curve of 0.82. For NYHA class III/IV, a cut-off BNP/ANP ratio of 2.97 produced a sensitivity of 78%, specificity of 87% and area under the ROC curve of 0.86 (Figure 4). The area under the ROC curve was higher for each of the BNP/ANP ratios than for levels of ANP and BNP, as well as the echocardiographic measures of the LVDd, LVDs and EF.

DISCUSSION

In the present study, ANP and BNP levels increased among all moderate or severe chronic MR cases. However, while ANP and BNP levels increased with the progression of heart failure symptoms, no increases were observed in NYHA class III/IV; in fact, ANP levels showed a decrease in this class. On the other hand, ANP and BNP levels showed no primary correlation with LV function measurements such as LAd, LV diameters and LVEF. Although ANP levels increased initially with atrial enlargement, they decreased when the enlargement became marked. Similarly, BNP levels tended to decrease with marked enlargement of the atrium. However, the BNP/ANP ratio increased with the progression of heart failure symptoms, decreased LV function and larger LAd.

Activation of the neurohormonal system is a self-compensatory mechanism against heart failure. Neurohormonal factors, such as the vasoconstrictors norepinephrine, renin and endothelin-1, play important roles in the pathogenesis of heart failure and have been reported to be prognostic predictors of heart failure (6-8). ANP and BNP are secreted from cardiomyocytes secondary to increased atrial and ventricular wall stretch. After release from the heart, the circulating natriuretic peptides bind to peripheral receptors, resulting in natriuresis, vasodilation, inhibition of the renin-angiotensin-aldosterone system and cardioprotection.

Little data are available on neurohormonal factors in valvular disorders, especially the kinetics of natriuretic peptides. In valvular disorders, ANP and BNP levels are affected by the site of valve damage (mitral, aortic, etc), the form of damage (regurgitation, stenosis), the severity of valve dysfunction (regurgitant fraction, effective orifice area), as well as ventricular and atrial function (9-13). Chronic LV volume overload as a result of MR leads to compensatory dilation of the LV. In addition, backflow into the LA results in enlargement of the LA, atrial fibrillation and pulmonary hypertension. MR is characterized by chronic volume overload and atrial fibrillation causing extensive degenerative change in the atrium (14,15). In MR, ANP and BNP levels are expected to vary depending on the severity and duration of individual cardiac cavity overload (10,11).

ANP is mainly stored as secretion granules in atrial myocardiocytes, and secretion is rapid (15). Overstretching of the atrial muscle and increased depolarization are proposed to be the stimuli for ANP secretion (16,17). Although ANP levels increase in atrial fibrillation, reports (18-21) have indicated that levels are lower among patients with atrial fibrillation of longer duration due to the degenerative change (atrophy and fibrosis) of atrial myocytes. In MR, chronic atrial overload and atrial fibrillation probably lower the ANP level.

BNP is a cardiac neurohormone specifically secreted from the ventricle in response to volume expansion and pressure overload (22-25). BNP is a truly ventricular hormone, and responds to changes in LV filling pressure. BNP may be a more sensitive and specific indicator of ventricular disorders than other natriuretic peptides (26,27). BNP level provides prognostic information independent of other variables previously associated with mortality and sudden death in patients with chronic heart failure, and is more useful than ANP or norepinephrine for predicting a poor prognosis (27,28).

BNP mRNA is expressed in atrial muscle, where BNP is also secreted; both have been reported to increase by atrial fibrillation and hypertrophy (24,29-32). Although the kinetics of atrial-derived BNP in heart failure are not fully known, some studies (23-25) propose that the atrium is the major source of secretion in the early stage of lowered cardiac function, and that BNP levels from the ventricle increase after the progression to heart failure. BNP and ANP are structurally similar, and BNP is probably also stored in secretion granules (16,33). Therefore, in chronic atrial fibrillation, it is likely that BNP secretion also decreases due to degeneration or atrophy and fibrosis of the atrial muscle, similar to ANP. In chronic MR, we speculate that despite an increase in levels of the mainly ventricle-derived BNP, the atrium-derived BNP levels may decrease when atrial damage becomes severe, and as a result, the net BNP level does not increase.

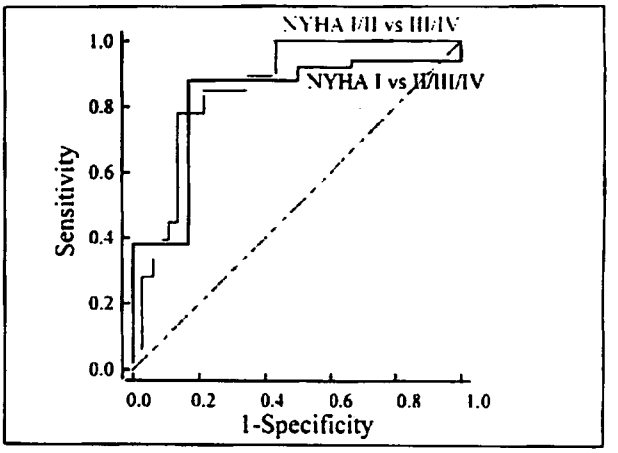

Figure 4) *Receiver-operating characteristic curves for the brain natriuretic peptide (BNP) to atrial natriuretic peptide (ANP) ratio to determine the severity for heart failure. Areas under the curve are 0.82 (New York Heart Association [NYHA] class I versus class II/III/IV) and 0.86 (NYHA class I/II versus class III/IV)*

Clinical implications

In practice, clinical decision on operative indication is most difficult for NYHA class II patients with mild symptoms. In the present study, ANP levels, BNP levels and the BNP/ANP ratios vary greatly in NYHA class II, probably reflecting a wide spectrum of disease conditions in this group. In clinical practice, assessment of symptoms may be difficult. It is likely that in some patients, the symptoms were not a consequence of MR, while others were classified as asymptomatic because they undertook little activity or neglected subtle symptoms. The results of the present study suggest that natriuretic peptide testing may add to the information obtained by echocardiography in the assessment of MR in clinical practice.

Limitations

BNP is mainly secreted in the ventricle, proportional to volume expansion and pressure overload (25). Cheung and Kumana (34) suggested that the BNP level reflects the long-term intravascular volume, rather than the momentary volume. On the other hand, Tsutamoto et al (27), Cheng et al (35) and Nakagawa et al (36) considered BNP to be an emergency hormone, responding instantaneously to ventricular volume overload. Unfortunately, we have little information on the stability or reproducibility of BNP levels measured over time in heart failure patients who have a stable course (37,38). In the present study, ANP and BNP levels were measured only once in the majority of patients. While changes in BNP level are supposed to reflect the pathology of heart failure, whether a single-baseline measurement determination during chronic heart failure accurately reflects the disease condition remains to be studied.

Much of the data in the present study highlight the ability of the BNP/ANP ratio to distinguish between NYHA class II to IV patients and class I patients. Unfortunately, we could only enrol eight class I patients in the study. Although the NYHA functional class was determined based on each patient's subjective symptoms, we could not obtain objective data, such as exercise oxygen uptake, to confirm patient functional status. Therefore, to elucidate the significance of the BNP/ANP ratio, future clinical studies that include more patients with mild MR and that collect exercise oxygen uptake data are needed.

CONCLUSION

The present study suggests that the BNP/ANP ratio is increased in chronic MR as a result of decreased ANP and BNP levels, which is due to atrial degeneration, as well as an increase in BNP levels, which is due to ventricular overload. In chronic MR, the levels of ANP and BNP, as well as the BNP/ANP ratio, are potential indicators of disease severity. A prospective study is needed to determine whether the BNP/ANP ratio can be used to predict mortality and morbidity in patients treated medically, and predict the postoperative course in those treated surgically.

REFERENCES

1. Corin WJ, Sütsch G, Murakami T, Krogmann O, Turina M, Hess OM. Left ventricular function in chronic mitral regurgitation: Preoperative and postoperative comparison. J Am Coll Cardiol 1995;25:113-21.
2. ACC/AHA guidelines for the management of patients with valvular heart disease. A report of the American College of Cardiology/American Heart Association. Task Force on Practice Guidelines (Committee on Management of Patients with Valvular Heart Disease). J Am Coll Cardiol 1998;32:1486-588.
3. Starling MR, Kirsh MM, Montgomery DG, Gross MD. Impaired left ventricular contractile function in patients with long-term mitral regurgitation and normal ejection fraction. J Am Coll Cardiol 1993;22:239-50.
4. Tribouilloy CM, Enriquez-Sarano M, Schaff HV, et al. Impact of preoperative symptoms on survival after surgical correction of organic mitral regurgitation: Rationale for optimizing surgical indications. Circulation 1999;99:400-5.
5. Helmcke F, Nanda NC, Hsiung MC, et al. Color Doppler assessment of mitral regurgitation with orthogonal planes. Circulation 1987;75:175-83.
6. Francis GS, Benedict C, Johnstone DE, et al. Comparison of neuroendocrine activation in patients with left ventricular dysfunction with and without congestive heart failure. A substudy of the Studies of Left Ventricular Dysfunction (SOLVD). Circulation 1990;82:1724-9.
7. Remes J, Tikkanen I, Fyhrquist F, Pyorala K. Neuroendocrine activity in untreated heart failure. Br Heart J 1991;65:249-55.
8. Swedberg K, Eneroth P, Kjekshus J, Wilhelmsen L. Hormones regulating cardiovascular function in patients with severe congestive heart failure and their relation to mortality. CONSENSUS Trial Study Group. Circulation 1990;82:1730-6.
9. Yoshimura M, Yasue H, Okumura K, et al. Different secretion patterns of atrial natriuretic peptide and brain natriuretic peptide in patients with congestive heart failure. Circulation 1993;87:464-9.
10. Sutton TM, Stewart RA, Gerber IL, et al. Plasma natriuretic peptide levels increase with symptoms and severity of mitral regurgitation. J Am Coll Cardiol 2003;41:2280-7.
11. Detaint D, Messika-Zeitoun D, Avierinos JF, et al. B-type natriuretic peptide in organic mitral regurgitation: Determinants and impact on outcome. Circulation 2005;111:2391-7.
12. Gerber IL, Stewart RA, Legget ME, et al. Increased plasma natriuretic peptide levels reflect symptom onset in aortic stenosis. Circulation 2003;107:1884-90.
13. Watanabe M, Murakami M, Furukawa H, Nakahara H. Is measurement of plasma brain natriuretic peptide levels a useful test to detect for surgical timing of valve disease? Int J Cardiol 2004;96:21-4.
14. Reed D, Abbott RD, Smucker ML, Kaul S. Prediction of outcome after mitral valve replacement in patients with symptomatic chronic mitral regurgitation. The importance of left atrial size. Circulation 1991;84:23-34.
15. Thiedemann KU, Ferrans VJ. Left atrial ultrastructure in mitral valvular disease. Am J Pathol 1977;89:575-604.
16. Hasegawa K, Fujiwara H, Itoh H, et al. Light and electron microscopic localization of brain natriuretic peptide in relation to atrial natriuretic peptide in porcine atrium. Immunohistocytochemical study using specific monoclonal antibodies. Circulation 1991;84:1203-9.
17. Nishimura K, Ban T, Saito Y, Nakao K, Imura H. Atrial pacing stimulates secretion of atrial natriuretic polypeptide without elevation of atrial pressure in awake dogs with experimental complete atrioventricular block. Circ Res 1990;66:115-22.
18. Van Den Berg MP, Crijns HJGM, Van Veldhuisen DJ, Van Gelder IC, De Kam PJ, Lie KI. Atrial natriuretic peptide in patients with heart failure and chronic atrial fibrillation: Role of duration of atrial fibrillation. Am Heart J 1998;135:242-4.
19. Sanfilippo AJ, Abascal VM, Sheehan M, et al. Atrial enlargement as a consequence of atrial fibrillation. A prospective echocardiographic study. Circulation 1990;82:792-7.
20. Seino Y, Shimai S, Ibuki C, Itoh K, Takano T, Hayakawa H. Disturbed secretion of atrial natriuretic peptide in patients with persistent atrial standstill: Endocrinologic silence. J Am Coll Cardiol 1991;18:459-63.
21. Yoshihara F, Nishikimi T, Sasako Y, et al. Plasma atrial natriuretic peptide concentration inversely correlates with left atrial collagen volume fraction in patients with atrial fibrillation: Plasma ANP as a possible biochemical marker to predict the outcome of the maze procedure. J Am Coll Cardiol 2002;39:288-94.
22. Ogawa Y, Nakao K, Mukoyama M, et al. Natriuretic peptides as cardiac hormones in normotensive and spontaneously hypertensive rats. The ventricle is a major site of synthesis and secretion of brain natriuretic peptide. Circ Res 1991;69:491-500.
23. Mukoyama M, Nakao K, Hosoda K, et al. Brain natriuretic peptide as a novel cardiac hormone in humans. Evidence for an exquisite dual natriuretic peptide system, atrial natriuretic peptide and brain natriuretic peptide. J Clin Invest 1991;87:1402-12.
24. Hystad ME, Geiran OR, Attramadal H, et al. Regional cardiac expression and concentration of natriuretic peptides in patients with severe chronic heart failure. Acta Physiol Scand 2001;171:395-403.
25. Luchner A, Stevens TL, Borgeson DD, et al. Differential atrial and ventricular expression of myocardial BNP during evolution of heart failure. Am J Physiol 1998;274:H1684-9.
26. Struthers AD. Prospects for using a blood sample in the diagnosis of heart failure. QJM 1995;88:303-6.
27. Tsutamoto T, Wada A, Maeda K, et al. Attenuation of compensation of endogenous cardiac natriuretic peptide system in chronic heart failure: Prognostic role of plasma brain natriuretic peptide concentration in patients with chronic symptomatic left ventricular dysfunction. Circulation 1997;96:509-16.
28. Berger R, Huelsman M, Strecker K, et al. B-type natriuretic peptide predicts sudden death in patients with chronic heart failure. Circulation 2002;105:2392-7.
29. Doyama K, Fukumoto M, Takemura G, et al. Expression and distribution of brain natriuretic peptide in human right atria. J Am Coll Cardiol 1998;32:1832-8.
30. Christoffersen C, Goetze JP, Bartels ED, et al. Chamber-dependent expression of brain natriuretic peptide and its mRNA in normal and diabetic pig heart. Hypertension 2002;40:54-60.
31. Murakami Y, Shimada T, Inoue S, et al. New insights into the mechanism of the elevation of plasma brain natriuretic peptide levels in patients with left ventricular hypertrophy. Can J Cardiol 2002;18:1294-300.
32. Inoue S, Murakami Y, Sano K, Katoh H, Shimada T. Atrium as a source of brain natriuretic polypeptide in patients with atrial fibrillation. J Card Fail 2000;6:92-6.
33. Thibault G, Charbonneau C, Bilodeau J, Schiffrin EL, Garcia R. Rat brain natriuretic peptide is localized in atrial granules and released into the circulation. Am J Physiol 1992;263:R301-9.
34. Cheung BMY, Kumana CR. Natriuretic peptides – relevance in cardiovascular disease. JAMA 1998;280:1983-4.
35. Cheng V, Kazanagra R, Garcia A, et al. Rapid transcriptional activation and early mRNA turnover of brain natriuretic peptide in cardiocyte hypertrophy. Evidence for brain natriuretic peptide as an "emergency" cardiac hormone against ventricular overload. J Am Coll Cardiol 2001;37:386-91.
36. Nakagawa O, Ogawa Y, Itoh H, et al. Rapid transcriptional activation and early mRNA turnover of brain natriuretic peptide in cardiocyte hypertrophy. J Clin Invest 1995;96:1280-87.
37. Maisel A. B-type natriuretic peptide levels: Diagnostic and prognostic in congestive heart failure: What's next? Circulation 2002;105:2328-31. (Erratum in 2002;106:387).
38. Tang WHW, Girod JP, Lee MJ, et al. Plasma B-type natriuretic peptide levels in ambulatory patients with established chronic symptomatic systolic heart failure. Circulation 2003;108:2964-6.